



Copper(I) and silver(I) complexes of anthraldehyde thiosemicarbazone: Synthesis, structure elucidation, in vitro anti-tuberculosis/cytotoxicity activity and interactions with DNA/HSA

Journal:	<i>Dalton Transactions</i>
Manuscript ID	DT-ART-09-2020-003104.R1
Article Type:	Paper
Date Submitted by the Author:	19-Oct-2020
Complete List of Authors:	<p>Khan, Ashiq; Lovely Professional University, Chemistry Paul, Kamal; Thapar Institute of Engineering and Technology, School of Chemistry and Biochemistry Brar, Iqbal; Thapar Institute of Engineering and Technology, School of Chemistry and Biochemistry Jasinski, Jerry P.; Keene State College Department of Chemistry, Department of Chemistry Smolenski, Victoria; Keene State College Hotchkiss, Ethan ; Keene State College, Department of Chemistry Kelley, Patrick ; Keene State College Shalit, Zachary ; Keene State College Kaur, Manpreet; Keene State College, Department of Chemistry Banerjee, Somesh; Indian Institute of Technology Roorkee, Biotechnology Roy, Partha ; Indian Institute of Technology Roorkee, Department of Biotechnology Sharma, Rekha; Lovely Professional University, Chemistry</p>

**Copper(I) and silver(I) complexes of anthraldehyde thiosemicarbazone:
Synthesis, structure elucidation, *in vitro* anti-tuberculosis/cytotoxicity
activity and interactions with DNA/HSA**

Ashiq Khan^a, Kamaldeep Paul^b, Iqbal Singh^b, Jerry P. Jasinski^c, Victoria A. Smolenski, Ethan P. Hotchkiss^c, Patrick T. Kelley^c, Zachary A. Shalit^c, Manpreet Kaur^c, Somesh Banerjee^d, Partha Roy^d, Rekha Sharma^{a,□}

^aDepartment of Chemistry, Lovely Professional University, Phagwara, Punjab, India

^bSchool of Chemistry and Biochemistry, Thapar Institute of Engineering & Technology, Patiala 147004, Punjab, India

^cDepartment of Chemistry, Keene State College, 229 Main Street, Keene, NH 03435–2001, US

^dDepartment of Biotechnology, Indian Institute of Technology Roorkee, Roorkee 247667, Uttarakhand

Abstract

Reaction of copper (I) halides (X = I, Br, Cl) and silver (I) halides with 9-anthraldehyde thiosemicarbazone (9-Hanttsc, H¹L) and triphenylphosphine formed halogen-bridged dinuclear complexes, [M₂(μ₂-X)₂(η¹-S-9-Hanttsc)₂(Ph₃P)₂] (M = Cu, X = Cl, **1**; Br, **2**; I, **3**; M = Ag, X = Cl, **4**; Br, **5**). The similar reaction of 9-anthraldehyde-*N*¹-methyl thiosemicarbazone (9-Hanttsc-*N*¹-Me, H²L) with Ph₃P and silver (I) halides yielded sulfur-bridged dimers, [Ag₂X₂(μ₂-S-9-Hanttsc-*N*¹-Me)₂(Ph₃P)₂] (X = Cl, **9**; Br, **10**), however with copper (I) halides insoluble compounds were formed, which on the addition of one extra mole of Ph₃P gave mononuclear complexes of formula, [CuX(η¹-S-9-Hanttsc-*N*¹-Me)(Ph₃P)₂] (X = Cl, **6**; Br, **7**; I, **8**). All of the complexes have been characterized by elemental analysis, NMR (¹H, ¹³C) and single crystal x-ray crystallography (**2**, **5**, **6**, and **9**). Both the ligands (H¹L, H²L) and their complexes (**1-10**) were tested for their anti-tubercular and anticancer activities. The interactions of the ligand and their complexes (copper and silver) with calf thymus DNA (ct-DNA) and human serum albumin (HSA) were examined through UV-visible and fluorescence spectroscopy. Results showed that copper complex **2** displayed strong interactions with ct-DNA and HSA having binding constant values of 6.66 × 10⁴ M⁻¹ and 3.28 × 10⁴ M⁻¹, respectively, followed by silver complex **10** which gave the binding constant values of 4.60 × 10⁴ M⁻¹ and 3.06 × 10⁴ M⁻¹, respectively. All of the complexes also showed good interactions with DNA in docking studies.

Introduction

A wide range of biological applications like antineoplastic, antimycobacterial, antibacterial, antifungal, antiviral, antimalarial, and anticancer exhibited by thiosemicarbazones, made these molecules of prime focus for the researchers [1-9]. Apart from biological applications, thiosemicarbazones are also well known for their variable binding modes [10-17], ion sensing ability [18-21], and catalytic properties [22-25]. It has been observed that biological applications of thiosemicarbazones generally get enhanced on forming complexes with metals as in aqueous solution as metals form cations and can bind with anionic biological molecules [26-30]. Metal ions can also form three dimensional configurations by coordinating with ligands, which can attach to a particular target molecule [31, 32]. A number of metal-complexes with thiosemicarbazones having either one aromatic ring or two fused aromatic rings are structurally characterized [10-17], but with three fused aromatic rings, X-ray structure of only one complex with ruthenium, $[(\eta^6\text{-}p\text{-cymene})\text{Ru}(\text{NS})\text{Cl}]^+$ (NS = 9-anthraldehyde N-methyl-thiosemicarbazone) is known till date [33]. In the present paper, complexes of 9-anthraldehyde thiosemicarbazone (H^1L , 9-Hanttsc) and 9-anthraldehyde- N^1 -methyl-3-thiosemicarbazone (H^2L , 9-Hanttsc- N^1 -Me) (Chart I) with copper(I) and silver(I) have been synthesized and tested for their anti-tubercular and anticancer activities. Ligands and their complexes have been characterized by elemental analysis, spectroscopy (IR, ^1H NMR, and ^{13}C NMR) and single-crystal X-ray crystallography (**2**, **5**, **6** and **9**). Ligands and their complexes **1-10** were tested for anti-tubercular activities and anticancer activity against human embryonic kidney cell line HEK 293. Further, ligand (H^2L), copper complexes (**2**, **6**, and **8**) and silver complexes (**9** and **10**) were evaluated for their interactions with DNA and HSA using UV-visible and fluorescence spectroscopy. Docking studies of the ligands and complexes were also performed with DNA.

Materials and methods

Potassium chloride, potassium bromide, potassium iodide, thiosemicarbazide, and triphenylphosphine were purchased from Loba Pvt. Ltd, whereas 9-anthraldehyde and 3-methylthiosemicarbazide were procured from Sigma Aldrich Chemicals Ltd and used without further purification. Copper(I) halides (I, Br, Cl) were synthesized using the literature method [34]. Silver halides (AgCl and AgBr) were prepared by mixing a solution of silver nitrates in methanol with a solution of potassium halides in methanol. Analysis of C, H, and N was obtained with a Thermoelectron FLASHEA1112 CHNS analyzer. Infrared spectra were recorded from KBr pellets in the range $4000\text{--}600\text{ cm}^{-1}$ on a SHIMADZU FTIR 8400S

spectrophotometer. ^1H and ^{13}C NMR were recorded on an AV500 FT spectrometer operating at a frequency of 500MHz and 125 MHz, respectively using CDCl_3 as the solvent with TMS as the internal standard. UV-Visible studies were carried out on a Shimadzu UV-2600 machine using a slit width of 1.0 nm and matched quartz cells. Emission spectra were determined on a Varian Cary Eclipse fluorescence spectrometer.

Synthesis of 9-anthraldehyde thiosemicarbazone (**H¹L**, 9-Hanttsc)

Thiosemicarbazide, (0.22 g, 2.42 mmol) was dissolved in 75ml of ethanol with heating. To it, 9-anthraldehyde (0.5 g, 2.42 mmol) was added and the mixture was refluxed for 5-6 hrs. The solution was filtered and kept for crystallization at room temperature. A yellow crystalline product was separated out after 3-4 days. Yellow needles, Yield, 85%, m.p, 163-165 °C. Melting point is low compare to the already reported due to the crystalline product obtained [35]. Main IR peaks (KBr, cm^{-1}): $\nu(\text{N-H})$, 3437s, 3271s; $\nu(-\text{NH}-)$, 3155m; $\nu(\text{C-H}_{\text{Ph}})$, 3030m; $\delta(\text{NH}_2) + \nu(\text{C=N}) + \nu(\text{C=C})$ 1670s, 1599s, 1487s; $\nu(\text{C=S})$ 846s (thioamide moiety). ^1H NMR (δ , ppm; J , Hz; CDCl_3): 10.43 s (1H, N^2H), 8.49 s (1H, N^1H), 9.05 s (1H, C^2H), 8.41 d (2H, $J = 12$ Hz, $\text{C}^{5,15}\text{H}$), 8.50 s (1H, C^{10}H), 8.41 d (2H, $J = 12$ Hz, $\text{C}^{5,15}\text{H}$), 8.00 d (2H, $J = 8$ Hz, $\text{C}^{8,12}\text{H}$), 7.68-7.66 m (4H, $\text{C}^{6,7,13,14}\text{H} + \text{N}^1\text{H}_2$). ^{13}C NMR (δ , ppm; CDCl_3): 179.0 (C^1), 142.7 (C^2), 131.4 (C^{16}), 130.4 (C^4), 130.3 (C^9), 129.4 (C^{11}), 129.2 (C^5), 127.4 (C^{15}), 130.2 (C^{10}), 130.0 (C^3), 129.1 (C^8), 128.6 (C^{12}), 127.6 (C^6), 125.6 (C^{14}), 124.6 (C^7), 124.2 (C^{13}).

Synthesis of 9-anthraldehyde- N^1 -methyl-3-thiosemicarbazone (**H²L**, 9-Hanttsc- N^1 -Me)

4-Methyl thiosemicarbazide, (0.25g, 2.42 mmol) was dissolved in 75ml of ethanol with heating. To it, 9-anthraldehyde (0.5g, 2.42 mmol) was added and the mixture was refluxed for 5-6 hrs. The solution was filtered and kept for crystallization at room temperature. Yellow crystalline product was separated out after 3-4 days. Yield, 84%, m.p, 145-147 °C; Main IR peaks (KBr, cm^{-1}): $\nu(\text{N-H})$ 3398s, 3207s; $\nu(-\text{NH}-)$ 3113s; $\nu(\text{C-H}_{\text{Ph}})$, 3039m; $\nu(\text{C-H}_{\text{Me}})$ 2933m; $\delta(\text{NH}_2) + \nu(\text{C=N}) + \nu(\text{C=C})$ 1620s, 1529s, 1489s; $\nu(\text{C=S})$ 840s (thioamide moiety). ^1H NMR (δ , ppm; J , Hz; CDCl_3): 9.71 s (1H, N^2H), 7.24 s (1H, N^1H), 8.89 s (1H, C^2H), 8.53 d (2H, $J = 8$ Hz, $\text{C}^{5,15}\text{H}$), 8.56 s (1H, C^{10}H), 8.06 d (2H, $J = 8$ Hz, $\text{C}^{8,12}\text{H}$), 7.57-7.47 m (4H, $\text{C}^{6,7,13,14}\text{H}$), 3.23 s (3H, $-\text{CH}_3$). ^{13}C NMR (δ , ppm; CDCl_3): 178.9 (C^1), 140.8 (C^2), 131 (C^{16}), 139.7 (C^4), 130.4 (C^9), 130.2 (C^{11}), 129.4 (C^{10}), 129.3 (C^3), 127.8 (C^5), 127.3 (C^8), 127.3 (C^{15}), 126.1 (C^{12}), 125.7 (C^{14}), 124.9 (C^6), 124.6 (C^7), 124.3 (C^{13}), 30.3 ($-\text{CH}_3$).

[Cu₂(μ_2 -Cl)₂(η^1 -S-9-Hanttsc)₂(Ph₃P)₂] (1). To a solution of CuCl (0.050 g, 0.50 mmol) in 15 ml of acetonitrile was added, 9-anthraldehyde thiosemicarbazone (0.08 g, 0.50 mmol). The

reaction mixture was stirred for 24 hours at room temperature. To it, solid Ph_3P (0.132 g, 0.50 mmol) was added and stirred for 5-10 minutes. A light green coloured solution thus obtained was filtered and kept for crystallization on slow evaporation at room temperature. Yield: 80%; m. p. 288-290 °C. Elemental analysis, Found: C, 63.77; H, 4.35; N, 6.55. $\text{C}_{68}\text{H}_{56}\text{Cl}_2\text{Cu}_2\text{N}_6\text{P}_2\text{S}_2$ requires 63.75; H, 4.37; N, 6.56. Main IR peaks (KBr, cm^{-1}), $\nu(\text{N-H})$, 3423s, 3244s; $\nu(-\text{NH}-)$, 3136m; $\delta(\text{NH}_2) + \nu(\text{C=N}) + \nu(\text{C-C})$, 1672s, 1562m, 1431s; $\nu(\text{C=S})$ 852s (thioamide moiety), $\nu(\text{P-C}_{\text{Ph}})$, 1095s. ^1H NMR (δ , ppm; CDCl_3): 12.34 s (1H, N^2H), 7.48 s (1H, N^1H_2) 9.32 s (1H, C^2H), 8.59-8.61 m (3H, $\text{C}^{5,10,15}\text{H}$), 7.56-7.50 m (2H, $\text{C}^{8,12}\text{H}$), 7.25-7.30 m (4H, $\text{C}^{6,7,13,14}\text{H} + \text{PH}_3\text{P}$). ^{13}C NMR (δ , ppm; CDCl_3): 175.9 (C^1), 147.4 (C^2), 131.9 (C^{16}), 134.8 (C^4), 130.2 (C^9), 130.6 (C^{11}), 133.6 (C^5), 131.6 (C^{15}), 129.8 (C^{10}), 129.3 (C^3), 128.9 (C^8), 128.8 (C^{12}), 127.8 (C^7), 127.4 (C^{13}), 125.9 (C^{14}), 124.1 (C^6).

Complexes **2** and **3** were also synthesized using the same procedure.

[Cu₂(μ_2 -Br)₂(η^1 -S-9-Hanttsc)₂(Ph₃P)₂] (2). Yield: 79%; m.p. 280-283 °C. Elemental analysis, Found: C, 59.61; H, 4.06; N, 6.15. $\text{C}_{68}\text{H}_{56}\text{Br}_2\text{Cu}_2\text{N}_6\text{P}_2\text{S}_2$ requires 59.60; H, 4.09; N, 6.13. Main IR peaks (KBr, cm^{-1}), $\nu(\text{N-H})$, 3449s, 3300s; $\nu(-\text{NH}-)$ 3139m; $\delta(\text{NH}_2) + \nu(\text{C=N}) + \nu(\text{C-C})$, 1628s, 1595m, 1468s; $\nu(\text{C=S})$ 852s (thioamide moiety), $\nu(\text{P-C}_{\text{Ph}})$, 1095s. ^1H NMR (δ , ppm; J , Hz; CDCl_3): 12.54 s (1H, N^2H), 7.08 s (1H, N^1H_2), 9.52 s (1H, C^2H), 8.01 d (2H, $J = 8$ Hz, $\text{C}^{5,15}\text{H}$), 8.49 d (1H, $J = 8$ Hz, C^{10}H), 7.56-7.50 m (2H, $\text{C}^{8,12}\text{H}$), 7.35-7.30 m (4H, $\text{C}^{6,7,13,14}\text{H}$). ^{13}C NMR (δ , ppm; CDCl_3): 175.4 (C^1), 146.4 (C^2), 131.2 (C^{16}), 134.2 (C^4), 130.7 (C^9), 130.6 (C^{11}), 133.2 (C^5), 131.4 (C^{15}), 129.9 (C^{10}), 129.2 (C^3), 128.8 (C^8), 128.7 (C^{12}), 127.8 (C^7), 127.3 (C^{13}), 125.7 (C^{14}), 124.9 (C^6).

[Cu₂(μ_2 -I)₂(η^1 -S-9-Hanttsc)₂(Ph₃P)₂] (3). Yield: 76%; m.p 280-283 °C. Elemental analysis, Found: C, 55.73; H, 3.85; N, 5.75. $\text{C}_{68}\text{H}_{56}\text{I}_2\text{Cu}_2\text{N}_6\text{P}_2\text{S}_2$ requires 55.77; H, 3.83; N, 5.74. Main IR peaks (KBr, cm^{-1}), $\nu(\text{N-H})$, 3444s, 3297s; $\nu(-\text{NH}-)$ 3147m; $\delta(\text{NH}_2) + \nu(\text{C=N}) + \nu(\text{C-C})$, 1651s, 1575m, 1476s; $\nu(\text{C=S})$ 852s (thioamide moiety), $\nu(\text{P-C}_{\text{Ph}})$, 1094s. ^1H NMR (δ , ppm; CDCl_3): 10.73 s (1H, N^2H), 6.97 s (1H, N^1H_2), 9.63 s (1H, C^2H), 7.68-7.61 m (3H, $\text{C}^{5,10,15}\text{H}$), 7.50-7.44 m (2H, $\text{C}^{8,12}\text{H}$), 7.68-7.66 m (4H, $\text{C}^{6,7,13,14}\text{H} + \text{PH}_3\text{P}$). ^{13}C NMR (δ , ppm; CDCl_3): 178.0 (C^1), 142.7 (C^2), 133.4 (C^{16}), 132.4 (C^4), 131.3 (C^9), 130.4 (C^{11}), 129.9 (C^5), 128.4 (C^{15}), 130.8 (C^{10}), 130.1 (C^3), 129.1 (C^8), 128.6 (C^{12}), 127.6 (C^6), 125.4 (C^{14}), 124.8 (C^7), 124.6 (C^{13}).

[Ag₂(μ_2 -Cl)₂(η^1 -S-9-Hanttsc)₂(Ph₃P)₂] (4). To a solution of AgCl (0.050 g, 0.34 mmol) in 15 ml of acetonitrile was added solid 9-anthraldehyde thiosemicarbazone (0.094 g, 0.34 mmol)

and the reaction mixture was stirred for 24 hrs at room temperature. To this was added solid Ph_3P (0.089 g, 0.34 mmol) and stirred for 5-10 minutes. A yellow coloured solution thus obtained was filtered and kept for crystallization on slow evaporation at room temperature. Yield: 69%; m.p 297-300 °C. Elemental analysis, Found: C, 59.6; H, 4.07; N, 6.15. $\text{C}_{68}\text{H}_{56}\text{Cl}_2\text{Ag}_2\text{N}_6\text{P}_2\text{S}_2$ requires 59.6; H, 4.09; N, 6.13. Main IR peaks (KBr, cm^{-1}), $\nu(\text{N-H})$, 3433s, 3296s; $\nu(-\text{NH}-)$ 3140m; $\delta(\text{NH}_2) + \nu(\text{C=N}) + \nu(\text{C-C})$, 1670s, 1537m, 1442m; $\nu(\text{C=S})$ 840s (thioamide moiety), $\nu(\text{P-C}_{\text{Ph}})$, 1066s. ^1H NMR (δ , ppm; J , Hz; CDCl_3): 12.35 s (1H, N^2H), 9.65 s (1H, C^2H), 8.44 d (2H, $J = 8$ Hz, $\text{C}^{5,15}\text{H}$), 8.51 d (1H, $J = 8$ Hz, C^{10}H), 8.11 d (2H, $J = 8$ Hz, $\text{C}^{8,12}\text{H}$), 7.79-7.73 m (4H, $\text{C}^{6,7,13,14}\text{H} + \text{N}^1\text{H}_2$). ^{13}C NMR (δ , ppm; CDCl_3): 173.7 (C^1), 148.9 (C^2), 135.6 (C^{16}), 135.1 (C^4), 134.4 (C^9), 133.4 (C^{11}), 130.9 (C^5), 130.7 (C^{15}), 132.2 (C^{10}), 131.7 (C^3), 129.9 (C^8), 129.0 (C^{12}), 128.1 (C^6), 128.9 (C^{14}), 127.2 (C^7), 127.9 (C^{13}).

Complex **5** was also synthesized using the same procedure

[Ag₂(μ_2 -Br)₂(η^1 -S-9-Hanttsc)₂(Ph₃P)₂] 5. Yield: 74%; m.p 278-280 °C. Elemental analysis, Found: C, 55.6; H, 3.87; N, 5.77. $\text{C}_{68}\text{H}_{56}\text{Br}_2\text{Ag}_2\text{N}_6\text{P}_2\text{S}_2$ requires 55.9; H, 3.84; N, 5.76. Main IR peaks (KBr, cm^{-1}), $\nu(\text{N-H})$, 3447s, 3281s; $\nu(-\text{NH}-)$ 3150m; $\delta(\text{NH}_2) + \nu(\text{C=N}) + \nu(\text{C-C})$, 1622s, 1594m, 1479s; $\nu(\text{C=S})$ 851s (thioamide moiety), $\nu(\text{P-C}_{\text{Ph}})$, 1094s. ^1H NMR (δ , ppm; J , Hz; CDCl_3): 12.40 s (1H, N^2H), 9.74 s (1H, C^2H), 8.52 d (2H, $J = 8$ Hz, $\text{C}^{5,15}\text{H}$), 8.52 d (1H, $J = 8$ Hz, C^{10}H), 8.31 d (2H, $J = 8$ Hz, $\text{C}^{8,12}\text{H}$), 7.71-7.63 m (4H, $\text{C}^{6,7,13,14}\text{H} + \text{N}^1\text{H}_2$). ^{13}C NMR (δ , ppm; CDCl_3): 175.7 (C^1), 146.9 (C^2), 134.3 (C^{16}), 134.1 (C^4), 132.4 (C^9), 132.4 (C^{11}), 130.4 (C^5), 130.3 (C^{15}), 132.7 (C^{10}), 131.4 (C^3), 129.0 (C^8), 128.9 (C^{12}), 128.7 (C^6), 128.6 (C^{14}), 127.5 (C^7), 127.4 (C^{13}).

[CuCl(η^1 -S-9-Hanttsc-N¹-Me)(Ph₃P)₂] (6). To a solution of CuCl (0.050 g, 0.50 mmol) in 15 ml of acetonitrile was added solid 9-anthraldehyde-*N*¹-methyl-3-thiosemicarbazones (0.087 g, 0.50 mmol) and the reaction mixture was stirred for 24 hrs at room temperature. To this was added solid Ph_3P (0.132 g, 0.50 mmol) and stirred for 5-10 min. A yellow coloured solution thus obtained was filtered and kept for crystallization on slow evaporation at room temperature. Yield: 78%; m.p. 256-258 °C. Elemental analysis, Found: C, 69.6; H, 4.93; N, 4.57. $\text{C}_{53}\text{H}_{45}\text{ClCuN}_3\text{P}_2\text{S}$ requires 69.4; H, 4.91; N, 4.58. Main IR peaks (KBr, cm^{-1}), $\nu(\text{N-H})$, 3316s, 3230m; $\nu(-\text{NH}-)$ 3123m; $\nu(\text{C-H}_{\text{Me}})$, 2961m; $\delta(\text{NH}_2) + \nu(\text{C=N}) + \nu(\text{C-C})$, 1624s, 1560m, 1479s; $\nu(\text{C=S})$ 840s (thioamide moiety), $\nu(\text{P-C}_{\text{Ph}})$, 1094s. ^1H NMR (δ , ppm; J , Hz; CDCl_3): 12.92 s (1H, N^2H), 9.39 s (1H, C^2H), 8.00 d (2H, $J = 8$ Hz, $\text{C}^{5,15}\text{H}$), 8.45 s (1H,

C¹⁰H), 8.06 d (2H, $J = 8$ Hz, C^{8,12}H), 7.53-7.63 m (4H, C^{6,7,13,14}H + N¹H + PPh₃), 3.78 t (3H, -CH₃). ¹³C NMR (δ , ppm; CDCl₃): 176.2 (C¹), 144.5 (C²), 134.4 (C¹⁶), 134.3 (C⁴), 134.2 (C⁹), 132.0 (C¹¹), 131.5 (C⁵), 130.4 (C¹⁵), 132.3 (C¹⁰), 131.5 (C³), 129.9 (C⁸), 125.6 (C¹²), 128.6 (C⁶), 128.5 (C¹⁴), 127.2 (C⁷), 125.3 (C¹³), 30.8 (-CH₃).

Complexes **7** and **8** were also prepared by similar methods.

[CuBr(η^1 -S-9-Hanttsc-N¹-Me)(Ph₃P)₂] (7). Yield: 77%; m.p. 262-264 °C. Elemental analysis, Found: C, 66.3; H, 4.67; N, 4.35. C₅₃H₄₅BrCuN₃P₂S requires 66.2; H, 4.68; N, 4.37. Main IR peaks (KBr, cm⁻¹), ν (N-H), 3383s, 3205s; ν (-NH-) 3124m; ν (C-H_{Me}), 2998m; δ (NH₂) + ν (C=N) + ν (C-C), 1621s, 1563m, 1433s; ν (C=S) 840s (thioamide moiety), ν (P-C_{Ph}), 1093s. ¹H NMR (δ , ppm; J , Hz; CDCl₃): 12.66 s (1H, N²H), 9.56 s (1H, C²H), 8.48 d (2H, $J = 2.8$ Hz, C^{5,15}H), 8.45 s (1H, C¹⁰H), 8.01 d (2H, $J = 8$ Hz, C^{8,12}H), 7.56-7.45 m (4H, C^{6,7,13,14}H + N¹H + PPh₃), 3.16 t (3H, -CH₃). ¹³C NMR (δ , ppm; J , Hz; CDCl₃): 175.2 (C¹), 145.3 (C²), 134.2 (C¹⁶), 134.1 (C⁴), 133.3 (C⁹), 132.8 (C¹¹), 131.5 (C⁵), 130.5 (C¹⁵), 130.0 (C¹⁰), 130.2 (C³), 129.1 (C⁸), 125.3 (C¹²), 128.9 (C⁶), 128.8 (C¹⁴), 127.4 (C⁷), 125.7 (C¹³), 30.3 (-CH₃).

[CuI(η^1 -S-9-Hanttsc-N¹-Me)(Ph₃P)₂] (8). Yield: 74%; m.p. 280-283 °C. Elemental analysis, Found: C, 63.3; H, 4.46; N, 4.15. C₅₃H₄₅ICuN₃P₂S requires 63.1; H, 4.46; N, 4.16. Main IR peaks (KBr, cm⁻¹), ν (N-H), 3377s, 3205s; ν (-NH-) 3140m; ν (C-H_{Me}) 2997m; δ (NH₂) + ν (C=N) + ν (C-C), 1631s, 1562m, 1433s; ν (C=S) 840s (thioamide moiety), ν (P-C_{Ph}), 1097s. ¹H NMR (δ , ppm; J , Hz; CDCl₃): 11.74 s (1H, N²H), 9.30 s (1H, C²H), 8.53 d (2H, $J = 8$ Hz, C^{5,15}H), 8.11 s (1H, C¹⁰H), 7.84 d (2H, $J = 8$ Hz, C^{8,12}H), 7.63-7.32 m (4H, C^{6,7,13,14}H + N¹H + PPh₃), 2.99 s (3H, -CH₃). ¹³C NMR (δ , ppm; CDCl₃): 176.9 (C¹), 144.9 (C²), 135.4 (C¹⁶), 134.6 (C⁴), 134.5 (C⁹), 132.8 (C¹¹), 131.6 (C⁵), 130.8 (C¹⁵), 132.4 (C¹⁰), 131.5 (C³), 129.8 (C⁸), 125.8 (C¹²), 128.4 (C⁶), 128.5 (C¹⁴), 127.8 (C⁷), 125.6 (C¹³), 31.8 (-CH₃).

[Ag₂Cl₂(μ_2 -S-9-Hanttsc-N¹-Me)₂(Ph₃P)₂] (9). To a solution of AgCl (0.050 g, 0.34 mmol) in 15 ml of acetonitrile was added solid 9-anthraldehyde-*N*¹-methyl-3-thiosemicarbazone (0.099 g, 0.34 mmol) and the reaction mixture was stirred for 24 hrs at room temperature. To this was added solid Ph₃P (0.089 g, 0.34 mmol) and stirred for 5-10 min. An orange coloured solution thus obtained was filtered and kept for crystallization on slow evaporation at room temperature. Yield: 77% m.p. 218-220 °C. Elemental analysis, Found: C, 63.3; H, 4.56; N, 6.29. C₇₀H₆₀Cl₂Ag₂N₆P₂S₂ requires 63.0; H, 4.50; N, 6.30. Main IR peaks (KBr, cm⁻¹), ν (N-H), 3435m, 3362s; ν (-NH-) 3109s; ν (C-H_{Me}), 2993m; δ (NH₂) + ν (C=N) + ν (C-C), 1668s,

1558s, 1479s; $\nu(\text{C}=\text{S})$ 844s (thioamide moiety), $\nu(\text{P}-\text{C}_{\text{Ph}})$, 1089s. ^1H NMR (δ , ppm; J , Hz; CDCl_3): 13.01 s (1H, N^2H), 9.74 s (1H, C^2H), 8.49 d (2H, $J = 8$ Hz, $\text{C}^{5,15}\text{H}$), 8.40 s (1H, C^{10}H), 7.93 d (2H, $J = 8$ Hz, $\text{C}^{8,12}\text{H}$), 7.53-7.45 m (4H, $\text{C}^{6,7,13,14}\text{H} + \text{N}^1\text{H} + \text{PPh}_3$), 3.18 s (3H, $-\text{CH}_3$). ^{13}C NMR (δ , ppm; CDCl_3): 175.8 (C^1), 143.3 (C^2), 134.4 (C^{16}), 134.3 (C^4), 132.3 (C^9), 132.0 (C^{11}), 130.6 (C^5), 130.5 (C^{15}), 130.5 (C^{10}), 130.4 (C^3), 129.1 (C^8), 129.0 (C^{12}), 127.8 (C^6), 125.5 (C^{14}), 125.3 (C^7), 125.2 (C^{13}), 30.2 ($-\text{CH}_3$).

Complex **10** was also prepared by a similar method.

$\text{Ag}_2\text{Br}_2(\mu_2\text{-S-9-Hanttsc-N}^1\text{-Me})_2(\text{Ph}_3\text{P})_2$ (10**)**. Yield: 77%; m.p. 240-242 °C. Found: C, 59.1; H, 4.19; N, 5.94. $\text{C}_{70}\text{H}_{60}\text{Br}_2\text{Ag}_2\text{N}_6\text{P}_2\text{S}_2$ requires 59.0; H, 4.21; N, 5.90. Main IR peaks (KBr, cm^{-1}), $\nu(\text{N}-\text{H})$, 3372s, 3219s; $\nu(-\text{NH}-)$ 3132m; $\nu(\text{C}-\text{H}_{\text{Me}})$, 2993m; $\delta(\text{NH}_2) + \nu(\text{C}=\text{N}) + \nu(\text{C}-\text{C})$, 1670s, 1521s, 1490s; $\nu(\text{C}=\text{S})$ 844s (thioamide moiety), $\nu(\text{P}-\text{C}_{\text{Ph}})$, 1094s. ^1H NMR (δ , ppm; J , Hz; CDCl_3): 13.00 s (1H, N^2H), 9.74 s (1H, C^2H), 8.59 d (2H, $J = 8$ Hz, $\text{C}^{5,15}\text{H}$), 8.40 s (1H, C^{10}H), 7.97 d (2H, $J = 8$ Hz, $\text{C}^{8,12}\text{H}$), 7.63-7.53 m (4H, $\text{C}^{6,7,13,14}\text{H} + \text{N}^1\text{H} + \text{PPh}_3$), 3.22 s (3H, $-\text{CH}_3$). ^{13}C NMR (δ , ppm; CDCl_3): 175.3 (C^1), 143.9 (C^2), 134.8 (C^{16}), 134.3 (C^4), 132.1 (C^9), 132.6 (C^{11}), 130.5 (C^5), 130.4 (C^{15}), 130.2 (C^{10}), 130.1 (C^3), 129.8 (C^8), 129.0 (C^{12}), 127.9 (C^6), 126.5 (C^{14}), 126.3 (C^7), 126.2 (C^{13}), 31.2 ($-\text{CH}_3$).

X-ray crystallography

Crystals of **2**, **5**, **6** and **9** were mounted on a Rigaku, Gemini Eos diffractometer. Data was collected with graphite monochromated Mo-K α radiation ($\lambda = 0.71073\text{\AA}$) for **2**, **5**, and **9**, whereas with graphite monochromated Cu-K α radiation ($\lambda = 1.54184\text{\AA}$) for complex **6**. The X-ray data (Table 5) for all the crystals were collected at 173°K. Structure solution of complexes were completed with ShelXT [36] and refinement was done with ShelXL [37]. Atomic scattering factors were taken from International Tables for Crystallography [38].

Anti-Tuberculosis Activity

The anti-mycobacterial activity of all of the compounds (ligands and their complexes) was assessed against *M. tuberculosis* using a Microplate Alamar Blue assay (MABA) [39]. This methodology is non-toxic, uses a thermally stable reagent, and shows a good correlation with the proportional and BACTEC radiometric method. Briefly, 200 μl of sterile deionized water was added to all outer perimeter wells of a sterile 96 well plate to minimize evaporation of the medium in the test wells during incubation. The 96 well plates received 100 μl of 2000 cfu/ml of organisms in Middle brook 7H9 broth and a serial dilution of the compounds was made directly on the plate. The final drug concentrations tested were between 100 and 0.2 $\mu\text{g/ml}$. Each test was carried in triplicate. Plates were covered and sealed with parafilm and incubated

at 37 °C for five days in sealed plastic bags with 5% CO₂ atmosphere. After this time, 25 µl of freshly prepared 1:1 mixture of Almar Blue reagent and 10% tween 80 was added to the plates and incubated for 24 hrs. The blue color in the well was interpreted as no bacterial growth, and pink color was scored as growth. Pyrazinamide, ciprofloxacin, and streptomycin were included as standard drugs. The acceptable ranges, (MIC) of the standard drugs were 3.125 µg/ml, 3.125 µg/ml, and 6.25 µg/ml, respectively.

Cytotoxicity Studies

Cell culture. HeLa (human cervical cancer), HCT-15 (human colon cancer), DU-145 (human prostate cancer), PA-1 (human ovarian cancer) and HEK-293 (human kidney; non-cancerous; control) cell lines were used to study the cytotoxic effect of complexes. The cell lines were purchased from the cell line repository of National Centre of Cell Sciences, Pune, India. HeLa, PA-1 and HEK-293 cell lines were maintained in DMEM-high glucose media, whereas HCT-15 and DU-145 cell lines were maintained in RPMI-1640 media (both from Himedia, Mumbai, India). The medium was supplemented with 10% fetal bovine serum (heat-inactivated) and 1% antibiotics (100 U/ml penicillin & 100 µg/ml streptomycin) (both from Gibco, Thermo Fischer Scientific, Waltham, MA, USA). The cells were maintained at 37 °C in a humidified incubator supplied with 5% CO₂.

MTT assay. The anticancer activity of designed compounds was determined by performing MTT (4, 5-dimethyl-2-yl)-2,5-diphenyltetrazolium bromide) assay as mentioned earlier. Initial screening for the anticancer activity of all compounds was performed at 10 µM concentration. For this, 5000 cells in 100 µl complete media per well were seeded in a 96 well plate and allowed to incubate for 24 h, following which the designed compounds were added in duplicate in respective complete media at 10 µM concentration. After incubation of 24 h, 10 µl of MTT dye (5 mg/ml) was added to each well and incubated for around 4 h. Then the media was replaced without disturbing the formazan crystals, and 100 µl DMSO was added to each well and incubated for 20 min. Then the absorbance was measured at 570 nm using a FLUOstar Optima plate reader (BMG Labtech, Ortenberg, Germany).

The percentage inhibition was calculated by using the formula:

$$= 100 - [(\text{Mean OD of treated cell} / \text{Mean OD of vehicle-treated cells}) \times 100]$$

The compounds which achieved cell death well above 50% were tested further for determining their IC₅₀ values. Again for this assay 5000 cells were added to each well with 100 µl of complete media per well in 96 well plate. The further procedure adopted was the

same as mentioned above except that the test compounds were added at varying concentrations. The IC₅₀ value was determined by nonlinear regression analysis [nonlinear regression (sigmoidal dose-response with variable slope)] using Graph Pad Prism, version 5.02 software (Graph Pad Software Inc., CA, USA).

DNA and HSA interaction studies.

Sample preparation. The stock solution of calf thymus (ct)-DNA (4×10^{-3} M) was prepared by dissolving the DNA in 10 mM Tris with 1 mM EDTA (pH 7.4) at room temperature. The ratio of absorbance at 260 nm and 280 nm was used to calculate the purity of the DNA solution. The concentration of the stock solution of DNA was measured taking the average extinction coefficient $6600 \text{ M}^{-1} \text{ cm}^{-1}$ of a single nucleotide at 260 nm. The stock solutions (10^{-3} M) of ligand (**H²L**), copper complexes (**2**, **6**, and **8**) and silver complexes (**9** and **10**) were prepared in DMSO. The stock solution of HSA (10^{-3} M) was prepared in distilled water.

UV-visible spectroscopic method. The ligand (**H²L**), copper complexes (**2**, **6** and **8**) and silver complexes (**9** and **10**) ($5 \mu\text{M}$, phosphate buffer pH 7.4, 298 K) were titrated with incremental addition of ct-DNA ($0\text{-}40 \mu\text{M}$ for **H²L**; $0\text{-}48 \mu\text{M}$ for **2**; $0\text{-}20 \mu\text{M}$ for **6**; $0\text{-}28 \mu\text{M}$ for **8**; $0\text{-}32 \mu\text{M}$ for **9**; and $0\text{-}30 \mu\text{M}$ for **10**).

The experiment for HSA interaction with ligand (**H²L**), copper complexes (**2**, **6**, and **8**) and silver complexes (**9** and **10**) was performed taking HSA ($10 \mu\text{M}$, phosphate buffer, pH 7.4, 298 K) and an incremental addition of compounds ($0\text{-}25 \mu\text{M}$). In both ct-DNA and HSA interactions studies, baseline corrections were carried out using a blank solution containing a phosphate buffer, and UV-visible spectra were noted in the range of 200-800 nm. Binding constants (K_b) were determined from the Benesi-Hildebrand equation (equation-1) [40].

$$\frac{A_0}{(A-A_0)} = \frac{\epsilon_f}{(\epsilon_b - \epsilon_f)} + \frac{\epsilon_f}{(\epsilon_b - \epsilon_f)K_b [\text{Analyte}]} \dots\dots\dots 1$$

Where A_0 is the initial absorbance of the free ligand or complex/HSA, A is the absorbance of the ligand or complex/HSA in the presence of the analyte (ct-DNA or complex), and ϵ_f and ϵ_b are molar extinction coefficients of the ligand or complex or HSA in its free and fully bound forms, respectively. The plot of $A_0/(A-A_0)$ versus $1/[\text{analyte}]$ was constructed using the titration data and linear fitting, and the value of K_b was determined by taking the ratio of the intercept to the slope.

Fluorescence studies. Ethidium bromide (EB) displacement assay was carried out by adding the ligand/complex to an EB-DNA complex solution. The ethidium bromide ($1 \mu\text{M}$) and ct-DNA ($10 \mu\text{M}$) were titrated with varying concentration of ligand (**H²L**), copper complexes (**2**,

6 and **8**) and silver complexes (**9** and **10**) (0-20 μM for **H²L**; 0-30 μM for **2**; 0-100 μM for **6**; 0-78 μM for **8**; 0-50 μM for **9** and 0-45 μM for **10**) in phosphate buffer (pH 7.4) at 298 K. The EB-DNA complex was excited at 520 nm and emission spectra were recorded between 200 nm and 800 nm.

For HSA studies, fluorescence spectral measurements were carried out for HSA (10 μM) with varying concentration of the ligand/complex (0-25 μM for **H²L**; 0-15 μM for **2**; 0-14 μM for **6**; 0-22 μM for **8**; 0-22 μM for **9** and 0-18 μM for **10**) in phosphate buffer (pH 7.4) at 298 K. All emission spectra for DNA and HSA studies were noted in the range of 200 to 800 nm. The excitation and emission slit widths have been maintained constant throughout the experiment. The Stern-Volmer equation (equation-2) was used to determine the quenching process and to calculate the quenching constants [41]

$$\frac{F_0}{F} = 1 + K_{sv} [\text{Analyte}] = 1 + K_q \tau_0 [\text{Analyte}] \text{-----}2$$

Where F_0 and F are the intensities of emission spectra of the ligand or complex/HSA in the absence (free form) and the presence of the analyte (ct-DNA or ligand/complex), respectively. The Stern-Volmer quenching constant (K_{sv}) which is considered to be a measure of the efficiency of fluorescence quenching by the analyte along with bimolecular quenching constants (K_q) were calculated from the plot of F_0/F versus [analyte].

The modified Stern-Volmer equation (equation-3) was used to get the values of the binding constant (K_b) and the average number of binding sites (n) [42].

$$\log \frac{F_0 - F}{F} = \log K_b + n \log [\text{analyte}] \text{-----}3$$

The parameters are the same as those of the Stern-Volmer equation. The binding constants (K_b) and the average number of binding sites (n) were calculated from the antilog of intercept and slope of the straight regression line, respectively, from the plot of $\log \{(F_0 - F)/F\}$ versus $\log [\text{analyte}]$.

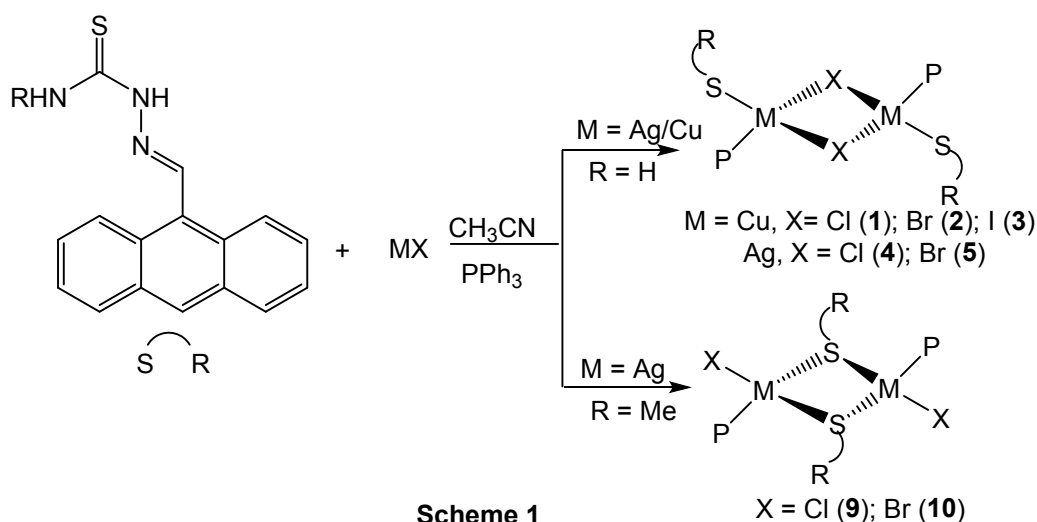
Docking Simulation

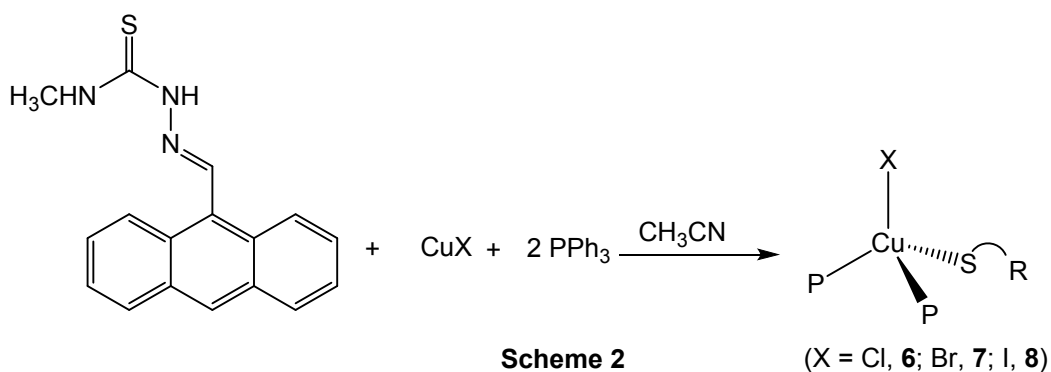
Molecular docking of the complexes into a 3-D X-ray structure of DNA (PDB: 1BNA) [43, 44] was carried out using the AutoDock software package (vina) [45]. The ligand structures in docking protocol were used as a crystal structure. The graphical user interface AutoDockTools (1.5.6rc3) was performed to set up every ligand DNA interaction, where all hydrogen atoms were added, gasteiger charges were calculated and nonpolar hydrogen atoms were merged to carbon atoms. The 3D structures of the ligand and metal complexes were optimized using the Gaussian 09W program and saved in pdb format. The partial charges of

pdb file were further modified by using the ADT package (version 1.5.6rc3) so that the charges of the nonpolar hydrogen atoms would be assigned to the atom to which the hydrogen is attached. The resulting file was saved as a Pdbqt file. The AutoDockTools program was used to generate the docking put files. In all docking, a grid box size of 44, 78, 106 pointing in x, y, and z directions were built. A grid spacing of 0.375 Å was used. Default settings were used with an initial population.

Synthesis

Schemes 1 and 2 give a pictorial view of the complexes synthesized. The reaction of copper (I) halides (X = I, Br, Cl) and silver (I) halides with 9-anthraldehyde thiosemicarbazone (9-Hantsc, H¹L) and triphenylphosphine in 1 : 1 : 1 (M : L : Ph₃P) molar ratio in acetonitrile yielded halogen-bridged dinuclear complexes, [M₂(μ₂-X)₂(η¹-S-9-Hanttsc)₂(Ph₃P)₂] (M = Cu, X = Cl, **1**; Br, **2**; I, **3**; M = Ag, X = Cl, **4**; Br, **5**) (**Scheme 1**). In contrast, the reaction of 9-anthraldehyde-*N*¹-methyl thiosemicarbazone with Ph₃P and silver (I) halides (1 : 1 : 1 molar ratio) formed sulfur-bridged dimers, [Ag₂X₂(μ₂-S-9-Hanttsc-*N*¹-Me)₂(Ph₃P)₂] (X = Cl, **9**; Br, **10**), whereas with copper (I) halides yielded an insoluble compound, which on the addition of one extra mole of Ph₃P formed a mononuclear complexes of formula, [CuX(η¹-S-9-Hanttsc-*N*¹-Me)(Ph₃P)₂] (X = Cl, **6**; Br, **7**; I, **8**) (**Scheme 2**). The substitution of hydrogen by a methyl group at the *N*¹ atom of the thiosemicarbazone has changed the bonding modes in its silver (I) complexes from halogen-bridging to sulphur-bridging and changed the nuclearity of its copper (I) complexes from dimers to monomers.





The $\nu(\text{N-H})$ band of H^1L and H^2L , appeared in the range, $3437 - 3207 \text{ cm}^{-1}$ due to symmetric and asymmetric stretching of the amino group and at $3155-3113 \text{ cm}^{-1}$ due to an amide group. In complexes **1-10**, these appeared in the ranges $3449-3205 \text{ cm}^{-1}$ and $3147-3123 \text{ cm}^{-1}$, respectively. Appearance of all the $\nu(\text{N-H})$ bands in these complexes ensured that no deprotonation occurred during complexation and that the thio- ligand coordinated in neutral form. The characteristic $\nu(\text{C=S})$ band of free ligands appeared at 846 cm^{-1} (H^1L) and 841 cm^{-1} (H^2L). These bands shifted to a high energy region in complexes **1-10** and appeared in the range $842-852 \text{ cm}^{-1}$.

The appearance of an additional band in the range, $1066-1094 \text{ cm}^{-1}$ due to $\nu(\text{P-C}_{\text{ph}})$ in complexes **1-10** ensured coordination of triphenylphosphine ligand to the metal center

Discussion on NMR spectroscopy

In ^1H NMR spectra $-\text{N}^2\text{H}-$ proton appeared in the range $\delta 10.73-13.01 \text{ ppm}$ in complexes **1-10** and showed a downfield shift vis-a-vis free ligands ($\delta 10.43 \text{ ppm}$ (H^1L), $\delta 9.71 \text{ ppm}$, H^2L). The appearance of $-\text{N}^2\text{H}-$ protons in these complexes ensured binding of the ligands in a neutral mode. Similarly, N^1H_2 protons in ligands H^5L and H^6L appeared at $\delta 8.49 \text{ ppm}$ and $\delta 7.24 \text{ ppm}$, respectively, however these peaks got obscured by the protons of the phenyl rings of anthraldehyde as well as triphenylphosphine in their complexes. Ring protons of anthraldehyde and phenyl rings of triphenylphosphine appeared in the range $\delta 8.11- 7.25 \text{ ppm}$. The presence of a methyl group at the N^1 atom of the thio- ligand was confirmed by the appearance of a peak in the range $\delta 3.16-3.78$ in complexes **6-10**.

The signal due to a C^1 atom in the ^{13}C NMR spectra of complexes **1-10** appeared in the range, $\delta 173.7-176.9 \text{ ppm}$, which are in the high field as compared to free ligands ($\delta 179.1$ (H^1L); $\delta 178.9$ (H^2L) ppm). The C^2 signals in complexes ($\delta 145.3-148.9 \text{ ppm}$) are at a low field relative to free ligands ($\delta 142.7$ (H^1L); 140.9 (H^2L) ppm). A methyl carbon at N^1 appeared in the range of $\delta 30.2-31.8 \text{ ppm}$ in complexes **6-10**.

Structure of dimers

Three dimers $[\text{Cu}_2(\mu_2\text{-Br})_2[(\eta^1\text{-S-9-Hanttsc})(\text{Ph}_3\text{P})_2]]$ **2**, $[\text{Ag}_2(\mu_2\text{-Br})_2(\eta^1\text{-S-9-Hanttsc})_2(\text{Ph}_3\text{P})_2]$ **5** and $[\text{Ag}_2\text{Cl}_2(\mu_2\text{-S-9-Hanttsc-N}^1\text{-Me})_2(\text{Ph}_3\text{P})_2]$ **9** crystallized in the triclinic crystal system with space group P-1. Molecular structures of these dimers are given in Figures 1-3, respectively. The crystallographic data and important bond parameters are given in Tables 1 and 2, respectively.

Each metal atom (Cu, **2**; Ag, **5**, **9**) is bonded to one P atom of triphenylphosphine, thione sulfur of the thiosemicarbazone, and one halogen atom (Br, **2**, **5**; Cl, **9**). Two such units are connected by a bromine bridge to form a central kernel, $\text{M}(\mu_2\text{-Br})_2\text{M}$ in **2**, and **5**, whereas by a thione sulphur to form the central kernel, $\text{Ag}(\mu_2\text{-S})_2\text{Ag}$ in **9**. Unequal M–X (Cu–Br, 2.4735(4), 2.5909(4) Å **2**; Ag–Br, 2.8086(3), 2.6534(3) Å **5**) and Ag–S (2.7761(7), 2.6007(7) Å **9**) bond lengths made the central kernel a parallelogram. Triphenylphosphine and a thio-ligand occupies a *trans*-orientation across the central kernel. The Cu–Br bond distances in **2** are slightly different from, {2.5425(5), 2.5892(5) Å} in $[\text{Cu}_2(\mu_2\text{-Br})_2(\text{HIntsc-N-Me})_2(\text{Ph}_3\text{P})_2]$ [27], $[\text{Cu}_2(\mu_2\text{-Br})_2(\text{Hbtsc})_2(\text{Ph}_3\text{P})_2]$ [46], {2.5275(3), 2.5771(2) Å} in $[\text{Cu}_2(\mu_2\text{-Br})_2(\text{Hbtsc-N-Me})_2(\text{Ph}_3\text{P})_2]$ and {2.5462(16), 2.5349(16) Å} in $[\text{Cu}_2(\mu_2\text{-Br})_2(\text{Hbtsc-N-Et})_2(\text{Ph}_3\text{P})_2]$ [47], similar to Ag–Br bond distances, {2.7210(3), 2.8115(3) Å} in $[\text{Ag}_2(\mu_2\text{-Br})_2(\text{Hbtsc})_2(\text{Ph}_3\text{P})_2]$ [48]. The C–S bond distances *ca.* 1.689–1.704 Å in dimers **2**, **5**, and **9** are less than C–S single bond (1.81 Å), but more than a C–S double bond (1.62 Å) indicating its a partial double bond character [49, 50].

Bond angles around the $\text{Cu}(\mu_2\text{-Br})_2\text{Cu}$ core (76.063 (12), 103.939(12)° in **2**) and $\text{Ag}(\mu_2\text{-Br})_2\text{Ag}$ core (71.079(9), 108.92(9)° in **5**) suggest that the geometry is distorted tetrahedral in these complexes, whereas angles within the $\text{Ag}(\mu_2\text{-S})_2\text{Ag}$ core, of 83.363(18)° and 96.631(19)° in **9** support nearly square planer geometry.

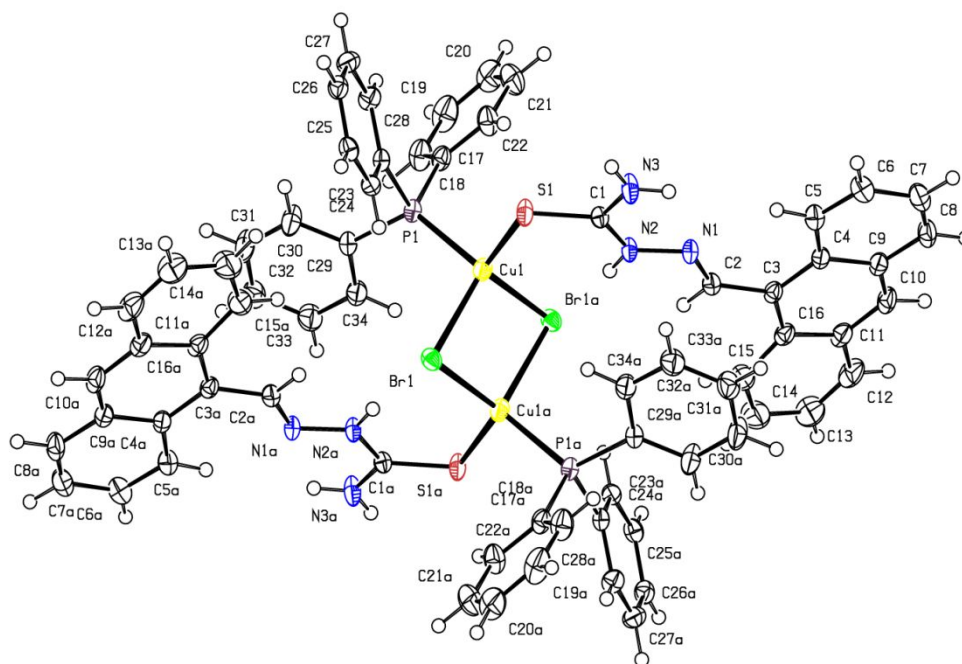


Figure 1. ORTEP view of $[\text{Cu}_2(\mu_2\text{-Br})_2][(\eta^1\text{-S-9-Hanttsc})(\text{Ph}_3\text{P})_2]$ **2** with the atom numbering scheme and 30% probability ellipsoids. Symmetry transformation (-x, -y, -z with inversion center at (0, 0, 0)). Ligands are bound to the metal are in an E geometric isomeric configuration.

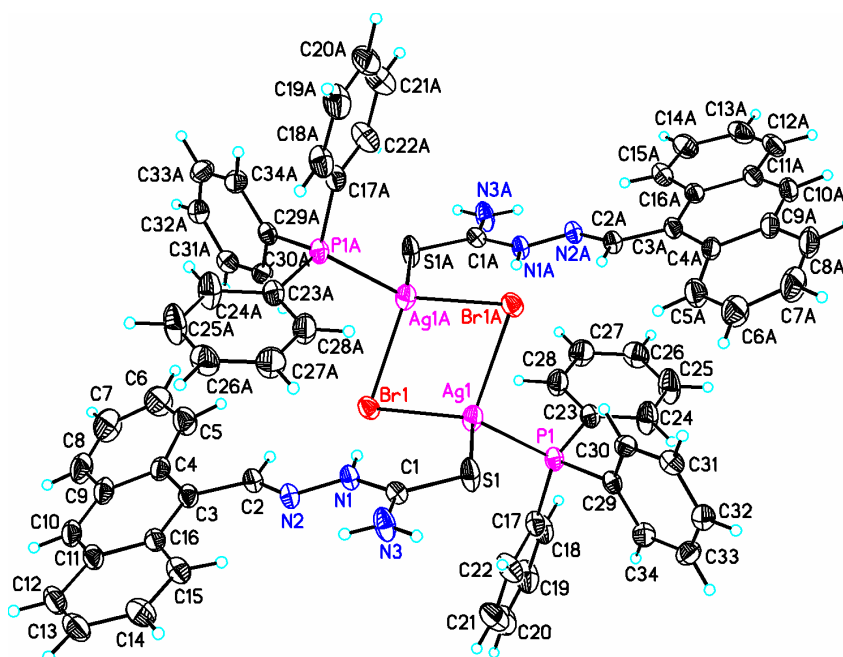


Figure 2. ORTEP view of $[\text{Ag}_2(\mu_2\text{-Br})_2][(\eta^1\text{-S-9-Hanttsc})(\text{Ph}_3\text{P})_2]$ **5** with the atom numbering scheme and 39% probability ellipsoids. Symmetry transformation (-x, -y, -z with inversion

center at (0, 0, 0)). Ligands are bound to the metal are in an E geometric isomeric configuration.

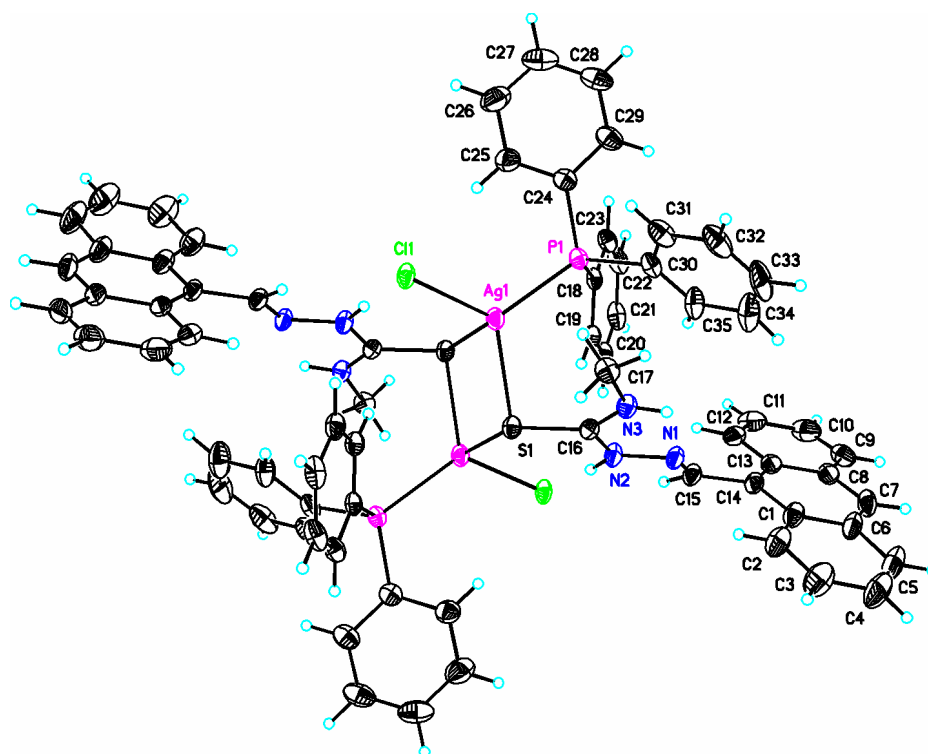


Figure 3. ORTEP view of $[\text{Ag}_2(\mu_2\text{-S-9-Hanttsc-N-Me})_2\text{Cl}_2(\text{Ph}_3\text{P})_2]$ **9** with the atom numbering scheme and 30% probability ellipsoids. Symmetry transformation $(-x, -y, -z)$ with inversion center at (0, 0, 0)). Ligands are bound to the metal are in an E geometric isomeric configuration.

Structure of monomer

Monomer **6** crystallized in the triclinic crystal system with space group P-1. Its molecular structure is given in Figure 4. The crystallographic data and important bond parameters are given in tables 1 and 2, respectively, along with complexes **2**, **5**, and **9**.

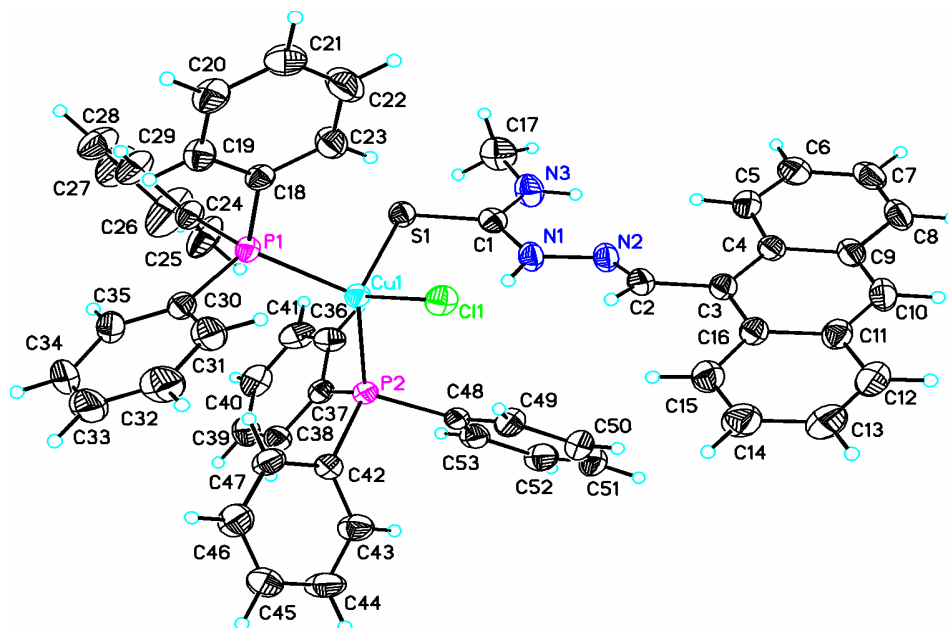


Figure 4. ORTEP view of $[\text{CuCl}(\eta^1\text{-S-9-Hanttsch-N}^1\text{-Me})(\text{Ph}_3\text{P})_2]$ **6** with the atom numbering scheme and 30% probability ellipsoids.

In complex **6**, one chlorine atom, two P atoms from two PPh_3 ligands and one thione S of the ligand occupy four corners of a tetrahedral configuration around the copper center. The Cu–S bond distance 2.3942 Å in **6** is close to other monomeric complexes of copper (I) with thiosemicarbazones reported in the literature [46]. The Cu–Cl bond distance of 2.3754(6) Å is less than the sum of ionic radii of Cu^+ and Cl^- (2.58 Å) [49]. The other bond distances, Cu–S (2.3942(5) Å) and Cu–P (2.2732(4), 2.2839(4) Å) are close to the literature value [40]. The C–S distance of 1.694(2) Å is longer than C=S (1.62 Å) and smaller than a C–S single bond (1.81 Å) indicating its partial double bond character in the metal complex [49, 50]. Bond angles around the copper atom in the range ca. 102.06(2)°– 109.65(2)° reveal distorted tetrahedral geometry with maximum distortion at the P–Cu–P bond angle (124.99(2)°).

Anti-tubercular activity

Anti-*M. Tuberculosis* activity of ligands (H^1L , H^2L) and their metal complexes (copper and silver) (**1–10**) were evaluated against the *M. Tuberculosis* H37RV strain ATCC 27294. Results for their Minimum Inhibitory Concentration (MIC) are given in Table 1. Standard drugs used for comparative analysis were streptomycin, ciprofloxacin, and pyrazinamide. Ligand H^1L was found to be active at 25 $\mu\text{g/ml}$ concentration, which got enhanced on complexation with Cu^{I} and Ag^{I} . The enhancement in anti-TB activity is much higher in complexes **1**, **4** and **5** (MIC = 1.65 $\mu\text{g/ml}$), even more than not only standard drugs, like

streptomycin (MIC = 6.25 $\mu\text{g/ml}$) ciprofloxacin (MIC = 3.125 $\mu\text{g/ml}$) and pyrazinamide (MIC = 3.125 $\mu\text{g/ml}$) used for comparison, but also in the “second line” drugs and some reported drugs *viz.*, clarithromycin (MIC = 8.0–16 $\mu\text{g/ml}$), tobramycin (MIC = 4.0–8.0 $\mu\text{g/ml}$) [51].

The anti-tuberculosis activity of H²L is quite high (MIC = 3.12 $\mu\text{g/ml}$) than H¹L. An increase in the hydrophilicity of H²L due to the presence of the methyl group at the N¹ atom of the thiosemicarbazone that could be one of the reasons for this enhanced activity. The anti-TB activity of H²L decreased on complexation (except for complex 7) in contrast to complexes 1-5.

Table 1. Anti-tuberculosis activity of synthesized compounds (H¹L, H²L, 1-10)

S. No	Compound	Mycobacterium tuberculosis H37RV strain							
		MIC ($\mu\text{g / mL}$)							
		100	50	25	12.5	6.25	3.12	1.6	0.8
1.	H ¹ L	S	S	S	R	R	R	R	R
2.	1	S	S	S	S	S	S	S	R
3.	2	S	S	S	S	S	R	R	R
4.	3	S	S	S	S	S	S	R	R
5.	4	S	S	S	S	S	S	S	R
6.	5	S	S	S	S	S	S	S	R
7.	H ² L	S	S	S	S	S	S	R	R
8.	6	S	S	S	R	R	R	R	R
9.	7	S	S	S	S	S	S	S	R
10.	8	S	S	S	S	S	R	R	R
11.	9	S	S	S	S	R	R	R	R
12.	10	S	S	S	S	R	R	R	R

S= Sensitive, R = Resistant

Anticancer activity

The anticancer activity of complexes 1-10 was evaluated against four different cancer cell lines. Initial cytotoxic screening at 10 μM confirmed that complexes 1-10; 4-10; 4, 5, 9, 10; 4,

9 had potent cytotoxic effect against PA-1, DU-145, HeLa, and HCT-15 cell lines, respectively (data not shown). These complexes were then selected further to evaluate the IC₅₀ values against respective cell lines. HEK-293 cell line was used as a control cell line. 5-fluorouracil (5-FU) was taken as a reference drug. IC₅₀ (μM) values of the selected complexes are presented in **Table 2**.

It has been observed that all complexes have a significant cytotoxic impact on human ovarian cancer cell line i.e., PA-1 with IC₅₀ value in the range of 6-9 μM for all complexes, whereas complexes **4-10** have IC₅₀ values in the range of 6-8 μM against human prostate cancer cell line (DU-145 cells). Complex **4, 5, 9** and **10** have IC₅₀ in the range of 6-7 μM against cervical cancer cell line (HeLa cells). Complex **4** and **9** have IC₅₀ around 6.8 μM against colon cancer cell line (HCT-15 cell). Interestingly, all the evaluated complexes showed IC₅₀ values comparable to that of 5-FU used as positive control. Taken together, it can be considered that the complexes **4** and **9** have the most effective anti-cancerous effect as evaluated in this study. The anti-cancer effect of other complexes is also considerable in respective cancerous condition since they all showed IC₅₀ values below 10 μM in most of the cell lines as tested by us. Also it is to be noted that most of the complexes (except **2** and **3**) did not affect the viability of non-cancerous HEK-293 cell line as indicated by very high IC₅₀ values which was in general close to or above 100 μM in this cell line.

Table 2. Cytotoxic activity (IC₅₀ values) of complexes **1-10** against different cell lines expressed as μM.

Complex	PA-1	DU-145	HeLa	HCT-15	HEK-293
[Cu ₂ (μ ₂ -Cl) ₂ (η ¹ -S- 9 -Hanttsc)(Ph ₃ P) ₂] (1)	8.156±.968	N.E.	N.E.	N.E.	331 ± 20.645
[Cu ₂ (μ ₂ -Br) ₂ (η ¹ -S- 9 -Hanttsc)(Ph ₃ P) ₂] (2)	9.107±0.098	N.E.	N.E.	N.E.	55.61 ± 4.321
[Cu ₂ (μ ₂ -I) ₂ (η ¹ -S- 9 -Hanttsc)(Ph ₃ P) ₂] (3)	6.906±0.107	N.E.	N.E.	N.E.	99.71 ± 11.254
[AgCl(η ¹ -S- 9 -Hanttsc)(Ph ₃ P) ₂] (4)	6.892±0.317	6.329±0.458	7.144±0.829	6.831±0.791	66.51 ± 4.257
[AgBr(η ¹ -S- 9 -Hanttsc)(Ph ₃ P) ₂] (5)	7.032±0.419	6.179±0.576	6.452±0.079	N.E.	169.9 ±

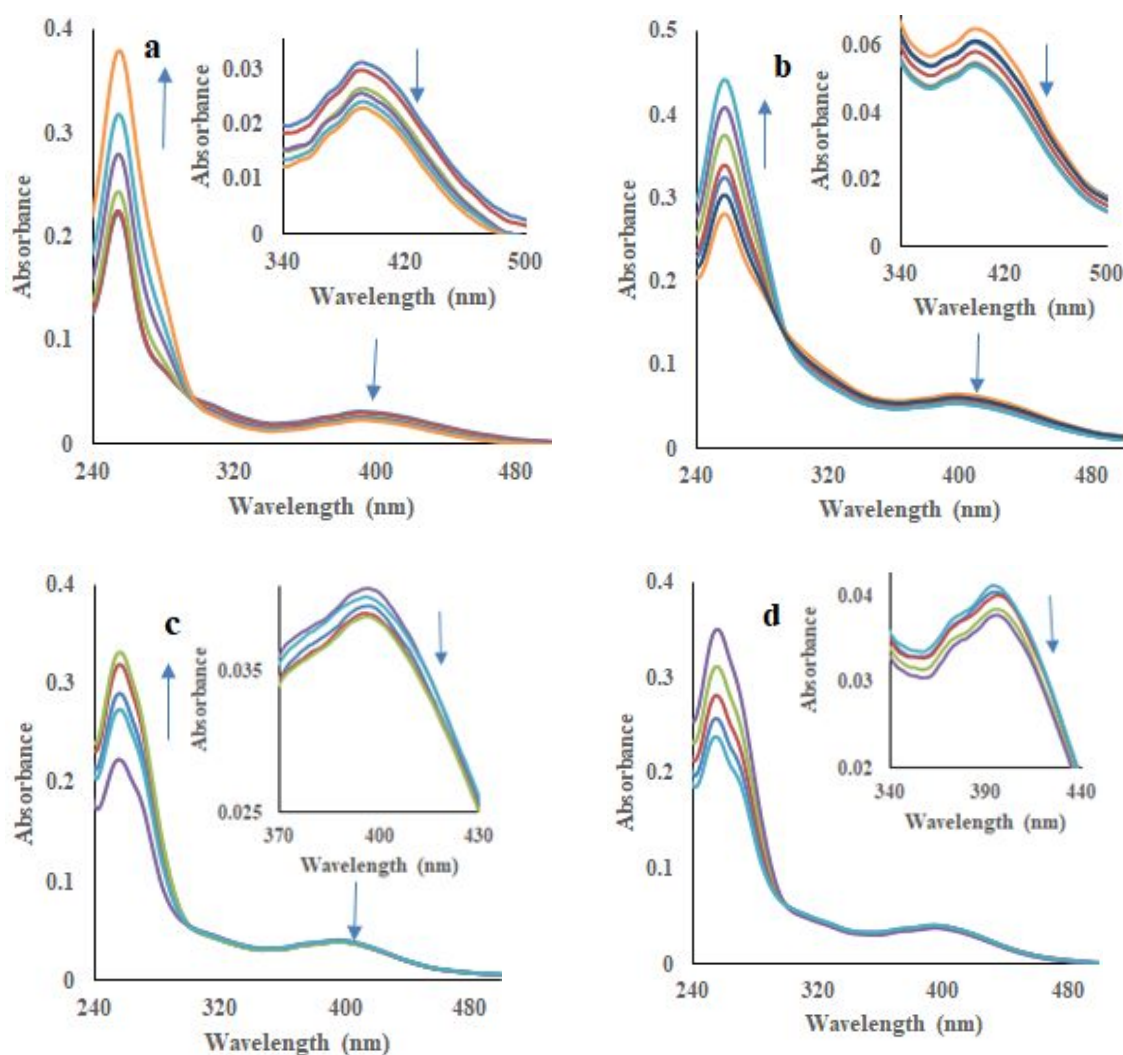
Hanttsc)(Ph₃P)₂] (5)						42.351
[CuCl(η^1 -S-9- Hanttsc-N ¹ - Me)(Ph ₃ P) ₂] (6)	7.138±0.616	7.692±0.432	N.E.	N.E.		238.1 ± 4.265
[CuBr(η^1 -S-9- Hanttsc-N ¹ - Me)(Ph ₃ P) ₂] (7)	7.411±0.106	6.024±0.509	N.E.	N.E.		283.8 ± 16.254
[CuI(η^1 -S-9- Hanttsc-N ¹ - Me)(Ph ₃ P) ₂] (8)	7.442±0.329	8.33±0.632	N.E.	N.E.		200.4 ± 23.254
[Ag ₂ Cl ₂ (μ_2 -S-9- Hanttsc-N ¹ - Me)(Ph ₃ P) ₂] (9)	6.681±0.710	6.024±0.509	6.964±0.311	6.868±0.239		197.8 ± 26.843
[Ag ₂ Br ₂ (μ_2 -S-9- Hanttsc-N ¹ - Me)(Ph ₃ P) ₂] (10)	6.292±0.089	6.251±0.301	6.292±0.291	N.E.		117.6 ± 31.257
Fluorouracil (5-FU)	8.25±0.7	15.4±0.78	2.08±0.22	12.2±0.51		145.56 ± 3.4

All numeric values represent Mean ± SEM (Standard Error of Mean) value of each evaluated complexes. N.E. represents Not Evaluated.

DNA interaction studies

UV-visible spectroscopic studies. Absorption spectroscopy is an effective technique to investigate the interaction mode of DNA with small molecules [40]. Thus, in order to provide evidence for the possibility of binding of copper and silver complexes to calf-thymus DNA, UV-visible titrations of a solution of the ligand and its complexes with ct-DNA have been performed. The absorption spectra of the ligand and its complexes were exhibited with absorption bands at 256 nm and 410 nm in a phosphate buffer (pH 7.4) at 298 K. The changes observed in the absorption spectra of ligand (**H²L**), copper complexes (**2**, **6** and **8**) and silver complexes (**9** and **10**) (5 μ M) with incremental addition of ct-DNA (0-40 μ M for **H²L**; 0-48 μ M for **2**; 0-20 μ M for **6**; 0-28 μ M for **8**; 0-32 μ M for **9**; and 0-30 μ M for **10**), showed hypochromic activity at 410 nm (29.03% for **H²L**; 20% for **2**; 5% for **6**; 7.31% for **8**; 7.31% for **9** and 13.23% for **10**) and hyperchromic activity at 256 nm (43.15% for **H²L**; 35.99% for

2; 33.93% for **6**; 33.61% for **8**; 19.53% for **9** and 12.29% for **10**) which indicates the interaction of these complexes with double-helical ct-DNA (**Figure 5**). The absorption intensity at 370 nm is decreased due to the fact that purine and pyrimidine bases of DNA are exposed because of the binding of complex moiety with DNA. To access the stability of an adduct formed between DNA and substrate, and based upon the variations in these absorption spectra, the Benesi-Hildebrand equation (equation-1) [39] has been used to calculate the intrinsic binding constants (K_b) for both the ligands and complexes and were found to be in the range of $1.40 - 6.66 \times 10^4 \text{ M}^{-1}$ (Figure S1, Table S1 of supplementary material). Complex **2** showed strongest interaction with a binding constant of $6.66 \times 10^4 \text{ M}^{-1}$, which is 4-5 times higher than that of ligand (H^2L). Results for the ligand and its complexes showed the binding interactions in the order of $\mathbf{2} > \mathbf{6} > \mathbf{8} > \mathbf{9} > \mathbf{10} > \text{H}^2\text{L}$.



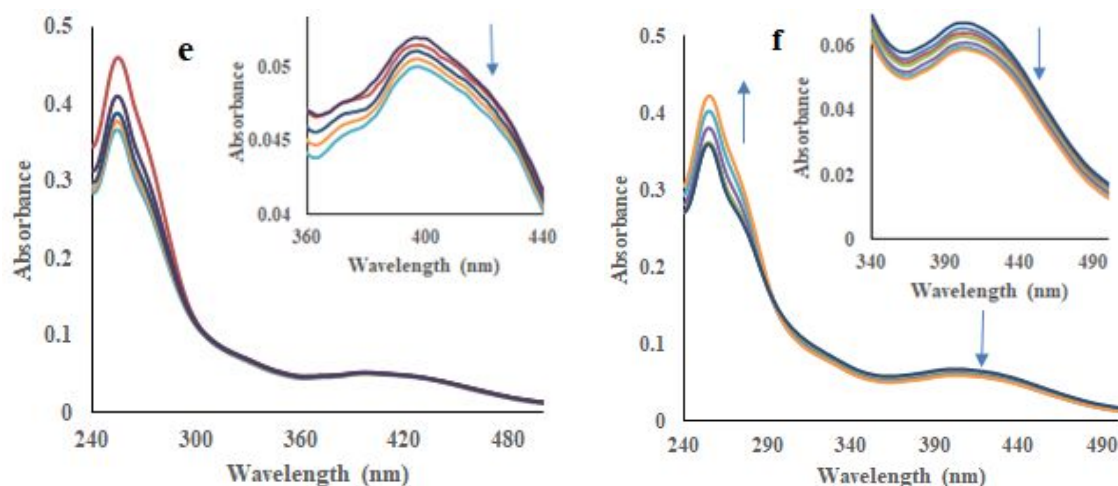


Figure 5. Absorption spectra of ligand ($10 \mu\text{M}$) H^2L (a), and complexes **2** (b); **6** (c); **8** (d); **9** (e) and **10** (f) with increasing concentrations of ct-DNA. Arrows (\uparrow) and (\downarrow) refer to hyperchromic and hypochromic effects, respectively.

Fluorescence studies. To investigate the mode of binding of a ligand (H^2L), copper complexes (**2**, **6**, and **8**) and silver complexes (**9** and **10**) to ct-DNA, a competitive binding experiment with ethidium bromide (EB) was performed. Ethidium bromide acts as one of the sensitive fluorescent probes having a planar structure that interacts with DNA by an intercalative binding mode [42]. Therefore, the relative affinity of ligand (H^2L), copper complexes (**2**, **6**, and **8**) and silver complexes (**9** and **10**) to DNA were compared by examining their ability to displace EB from the DNA helix. Ethidium bromide shows an emission maximum at 600 nm on excitation at its absorption maximum of 520 nm. Fluorescence spectra of a fixed concentration of the EB-DNA complex ($1 \mu\text{M} : 3 \mu\text{M}$) in the presence of increasing concentrations of ligand (H^2L), copper complexes (**2**, **6** and **8**) and silver complexes (**9** and **10**) ($0\text{-}20 \mu\text{M}$ for H^2L ; $0\text{-}30 \mu\text{M}$ for **2**; $0\text{-}100 \mu\text{M}$ for **6**; $0\text{-}78 \mu\text{M}$ for **8**; $0\text{-}50 \mu\text{M}$ for **9** and $0\text{-}45 \mu\text{M}$ for **10**) in phosphate buffer ($\text{pH } 7.4$) at 298 K were recorded (Figure 6). On subsequent addition of the ligand and the complexes, a decrease in fluorescence emission (11.18% for H^2L ; 58.07% for **2**; 22.07% for **6**; 51.55% for **8**; 21.63% for **9** and 42.10% for **10**) at 600 nm of EB-DNA complex was observed indicating that these complexes were effectively competing with EB for the occupation of the same binding sites on DNA through intercalation.

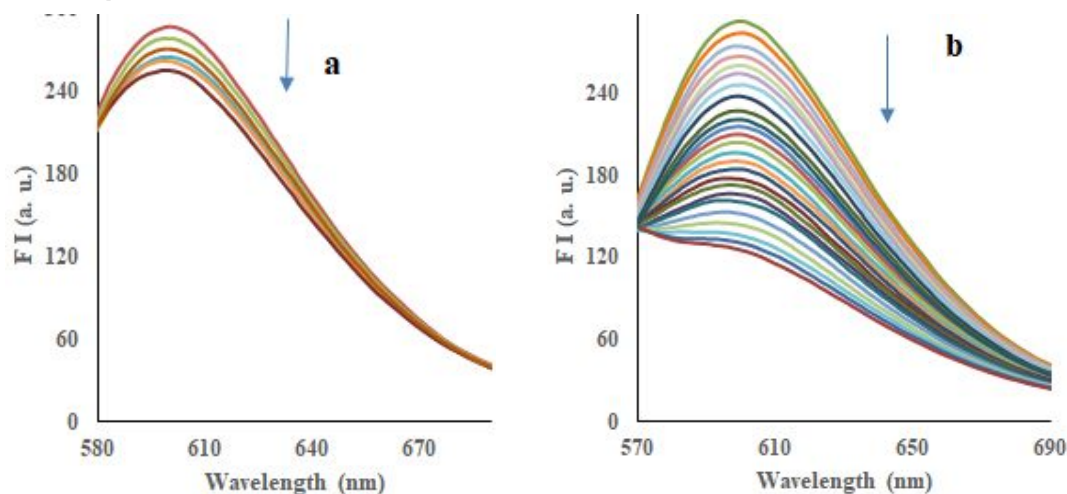
Quantitative estimation of the quenching with ligand (H^2L), copper complexes (**2**, **6** and **8**) and silver complexes (**9** and **10**) in terms of fluorescence quenching data were done by the Stern-Volmer equation (equation 2) [43], where K_{sv} and K_{q} have been calculated (Table

3, Figure S2 of supplementary material). The K_q is much larger than diffusion-controlled ($1.0 \times 10^{10} \text{ M}^{-1} \text{ s}^{-1}$) [45], also suggesting that interaction involves static quenching. Binding constants (K_b) and the average number of binding sites (n) per EB-DNA complex of the ligand or the complex interactions were calculated using the modified Stern-Volmer equation (equation 3) [42] (Figure S3 of supplementary material). The value of n was obtained from the slope which was found to be close to one.

Table 3. Quenching and binding parameters of ligand and complexes upon interaction with EB-ct-DNA complex

Comp.	$K_{SV} (\times 10^4) (\text{M}^{-1})$	$K_q (\times 10^{12}) (\text{M}^{-1}\text{s}^{-1})$	aR	$K_b (\times 10^4 \text{ M}^{-1})$	n	bR
H²L	0.52	0.52	0.9697	0.03	0.72	0.9673
2	1.02	1.02	0.9560	10.36	1.23	0.9822
6	1.35	1.35	0.9893	1.14	1.00	0.9930
8	1.26	1.26	0.9794	1.25	1.00	0.9882
9	0.60	0.60	0.9746	2.40	1.14	0.9883
10	1.13	1.13	0.9926	3.14	1.11	0.9926

aR (K_{SV} and K_q) and bR (K_b and n) are the correlation coefficients



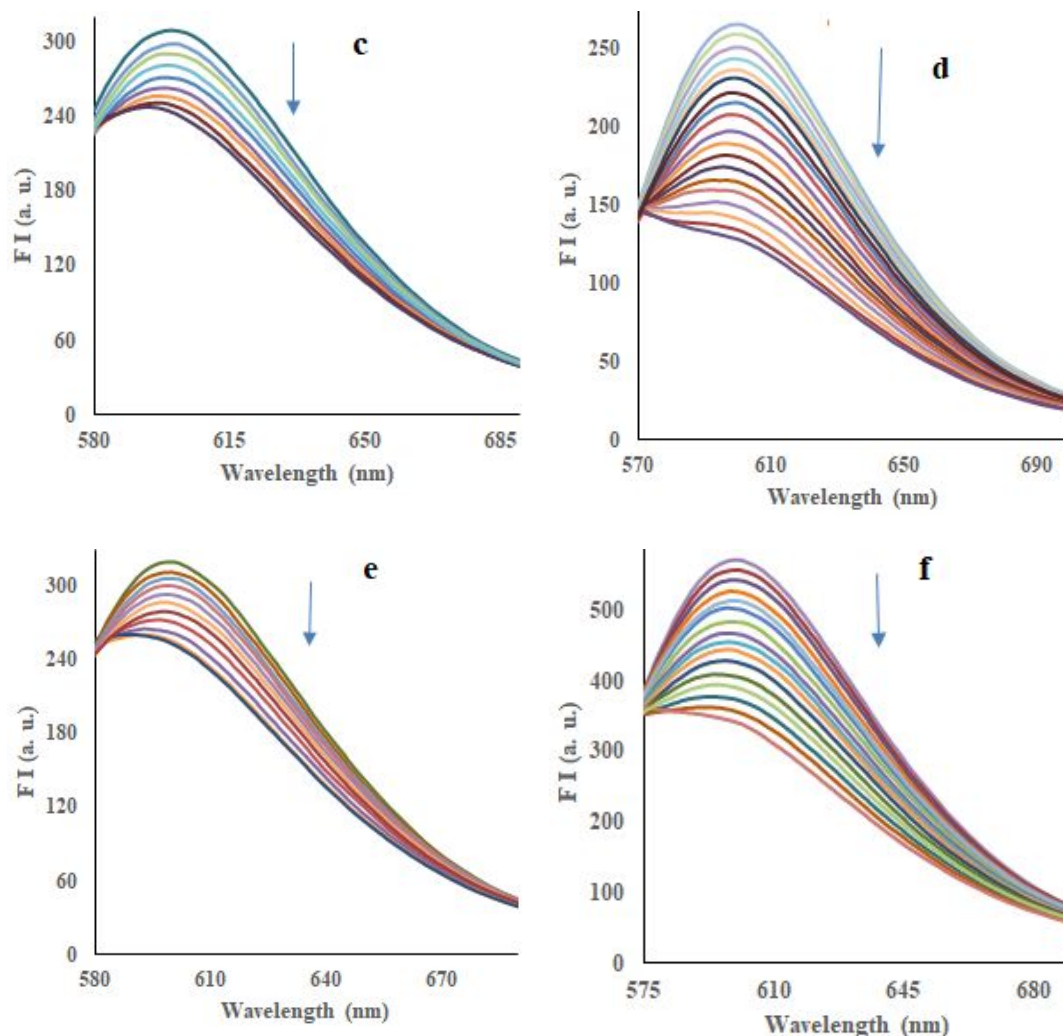
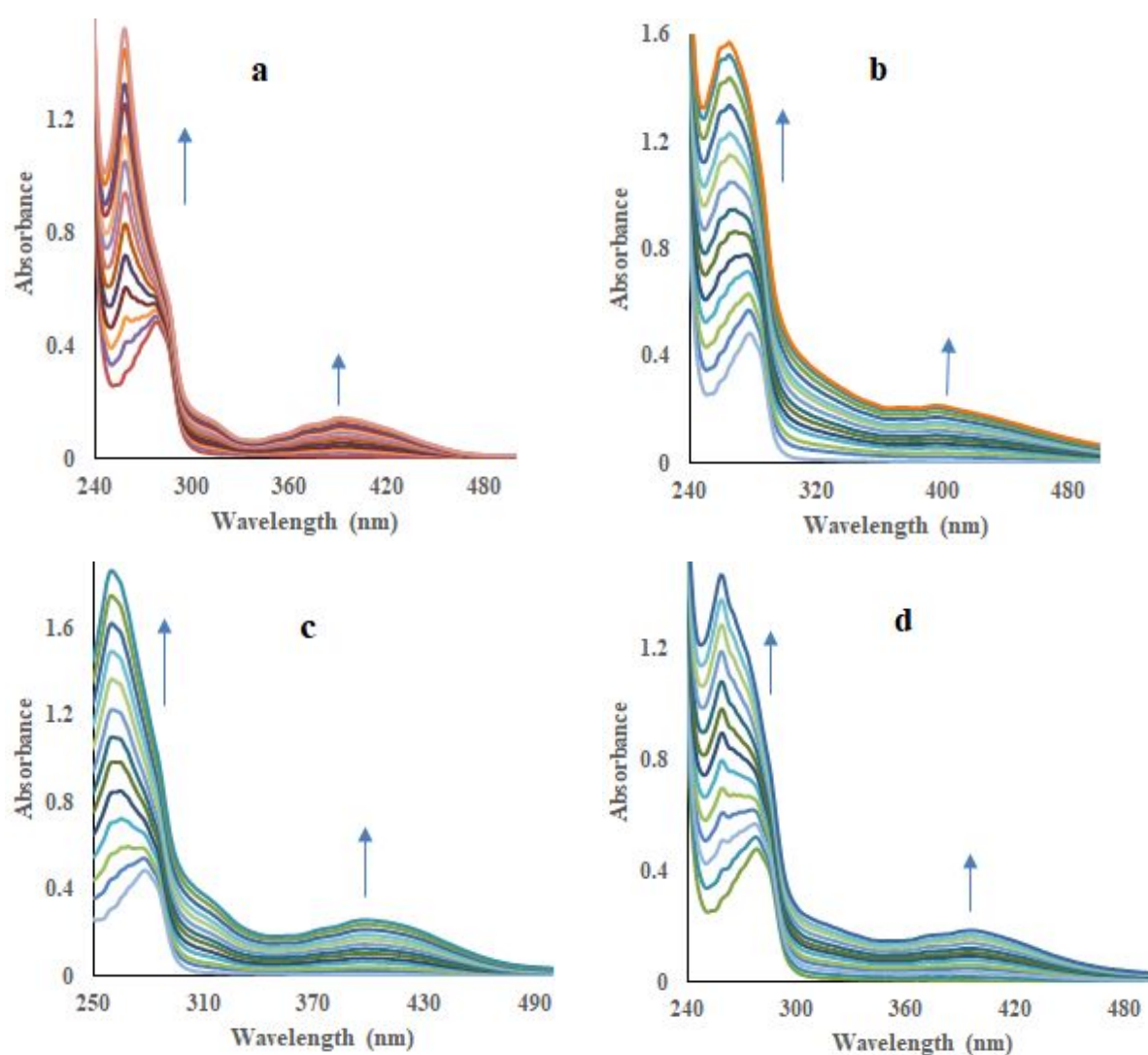


Figure 6. Emission spectra of EB ($1 \mu\text{M}$) bound to ct-DNA ($10 \mu\text{M}$) in the absence and increasing concentrations of the ligand **H²L** (a), and complexes **2** (b); **6** (c); **8** (d); **9** (e) and **10** (f). The arrow (\downarrow) shows a reduction of intensity on the concentration of the complex at room temperature.

HSA binding studies

UV-visible spectroscopic studies. Absorption spectroscopy is used to explore the possibility of ground state interaction between drug and protein [43]. Therefore, the interactions of derivatives with proteins have been inferred from the changes in absorption spectra of serum albumin with the gradual addition of the ligand and complexes. The UV-visible spectrum of HSA showed an intense absorption band at about 279 nm in a phosphate buffer (pH 7.4) at 298 K mainly due to the presence of tyrosine (Tyr), tryptophan (Trp) and phenylalanine (Phe) residues [52]. On subsequent addition of ligand (**H²L**), copper complexes (**2**, **6** and **8**) and silver complexes (**9** and **10**) (0 - $25 \mu\text{M}$) to HSA solution ($10 \mu\text{M}$), resulted in an excellent increase in intensity of the band at 279 nm (46.66% for **H²L**; 75% for **2**; 70.32% for **6**;

68.23% for **8**; 74.20% for **9** and 78.48% for **10**) with the appearance and enhancement of a new band at 395 nm corresponding to the complexes (Figure 7). Binding constants (K_b) for the interaction of the ligand and complexes with HSA has been calculated from the ratio of the intercept to the slope of the plot $1/(A-A_0)$ versus $1/[\text{ligand/complex}]$ using the Benesi-Hildebrand equation (equation 1) [41] and were found to be in the range of $0.50 - 3.28 \times 10^5 \text{ M}^{-1}$ (Table S2, Figure S4 of supplementary material). Complex **2** showed the strongest interaction with a binding constant of $3.28 \times 10^5 \text{ M}^{-1}$, which is 6-7 times higher than that of ligand (H^2L). The results for the ligand and complexes showed the binding interactions in the order of $2 > 6 > 8 > 9 > 10 > \text{H}^2\text{L}$.



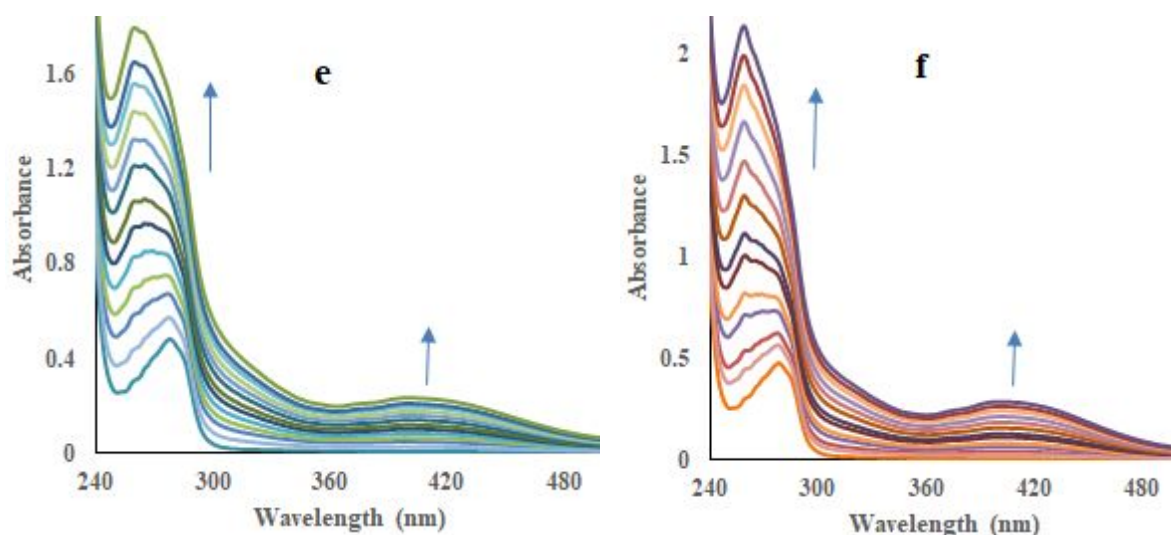


Figure 7. Absorption spectra of HSA ($10 \mu\text{M}$) with increasing concentrations of ligand **H²L** (a), and complexes **2** (b); **6** (c); **8** (d); **9** (e) and **10** (f). Arrows (\uparrow) refer to hyperchromic effects.

Fluorescence studies. The observations obtained from absorption studies are not sufficient to determine the interaction of the ligand/complexes in detail. Therefore, emission spectroscopy has been preferred for reviewing the binding mode of interactions. The fluorescence of HSA comes from two Trp residues; one of them is located on the surface and the other residue present in the hydrophobic pocket of the protein molecule [52]. Figure 8 depicts that on progressive addition of various concentration of the ligand and complexes ($0\text{--}25 \mu\text{M}$ for **H²L**; $0\text{--}15 \mu\text{M}$ for **2**; $0\text{--}14 \mu\text{M}$ for **6**; $0\text{--}22 \mu\text{M}$ for **8**; $0\text{--}22 \mu\text{M}$ for **9** and $0\text{--}18 \mu\text{M}$ for **10**), the emission spectrum of the Trp residues of serum protein at around 350 nm was gradually quenched (80.39% for **H²L**; 90.06% for **2**; 87.35% for **6**; 83.57% for **8**; 88.79% for **9**; and 90.43% for **10**) in aqueous phosphate buffer of $\text{pH } 7.4$ at 298 K with $\lambda_{\text{exc}} = 280 \text{ nm}$.

The steady-state fluorescence quenching in serum albumins with the addition of ligand/complexes can be characterized by the Stern-Volmer equation (equation 2) [43] that showed the relation between the quenching extent for each complex and the strength of their interactions with HSA. Values of the Stern-Volmer constant (K_{SV}) and bimolecular quenching constant (K_{q}) were calculated from the slope of the linear portion of the regression curve using equation 2 (Table 4, Figure S5 of supplementary material). A linear Stern-Volmer plot was obtained with the ligand and complexes suggesting that solely one type of quenching or binding process occurs, either static or dynamic quenching. The values obtained for bimolecular quenching constants (K_{q}) of the ligand and complexes ($1.99 - 15.60 \times 10^{13} \text{ M}^{-1}\text{s}^{-1}$)

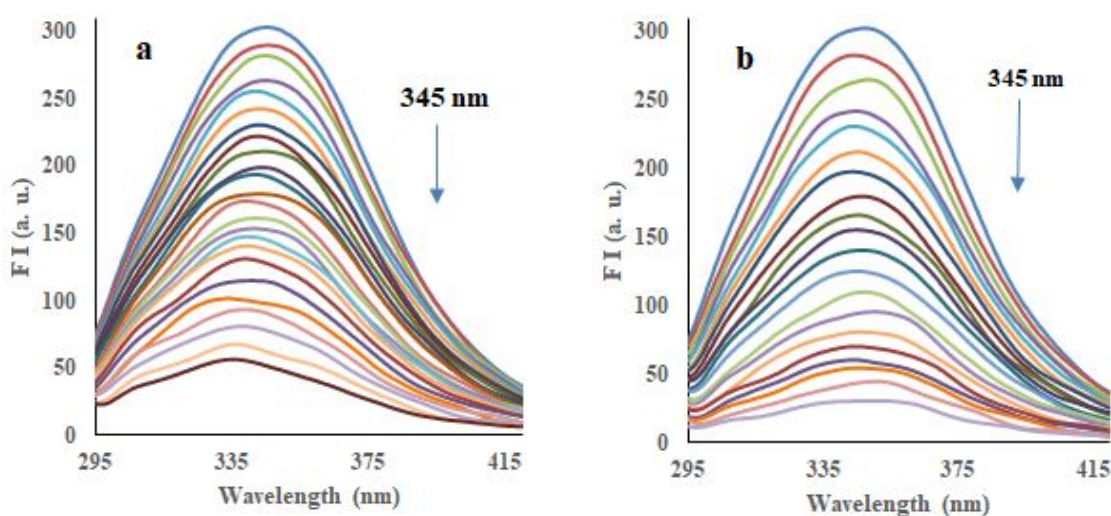
was found to be much greater than the diffusion control limited value of $1 \times 10^{10} \text{ M}^{-1} \text{ s}^{-1}$ [53], which is the largest possible value reported in an aqueous medium. Thus, the binding of the complexes to HSA probably involves the static quenching with the formation of the complex at the ground state.

The Modified Stern-Volmer equation (equation 3) [42] has been used to determine the binding constants (K_b) and the average number of binding sites (n) (Table 4) for the metal complexes-HSA from the corresponding $\log (F_0-F)/F$ versus $\log [\text{complex}]$ plot (Figure S6 of supplementary material). These complexes exhibited excellent binding parameters, suggesting their binding to the albumins and their possible transfer ability at their target sites similar to literature report [54].

Table 4. Quenching and binding parameters of ligand and metal complexes upon interactions with HSA

Comp.	$K_{SV} (\times 10^5) (\text{M}^{-1})$	$K_q (\times 10^{13}) (\text{M}^{-1} \text{s}^{-1})$	aR	$K_b (\times 10^6 \text{ M}^{-1})$	n	bR
H²L	1.99	1.99	0.9965	0.22	1.01	0.9867
2	15.60	15.60	0.9765	14.09	1.29	0.9970
6	5.45	5.45	0.9878	2.75	1.17	0.9992
8	2.22	2.22	0.9844	1.49	1.20	0.9977
9	7.83	7.83	0.9662	3.84	1.24	0.9961
10	9.06	9.06	0.9738	3.88	1.21	0.9933

aR (K_{SV} and K_q) and bR (K_b and n) are the correlation coefficients



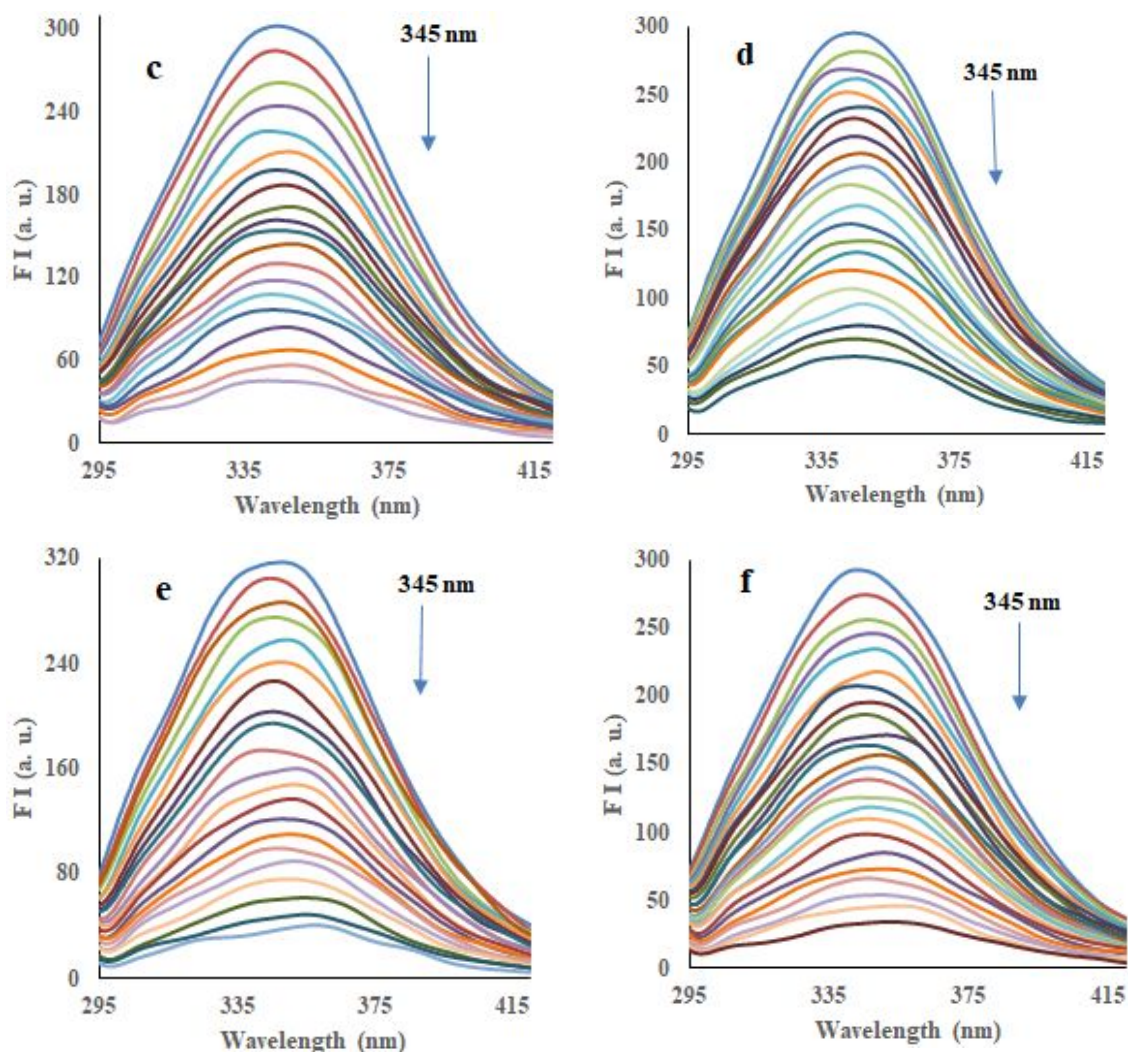


Figure 8. Emission spectra of HSA ($10 \mu\text{M}$) in the absence and increasing concentrations of the ligand H^2L (a), and complexes **2** (b); **6** (c); **8** (d); **9** (e) and **10** (f). The arrow (\downarrow) shows a reduction of intensity on the concentration of the complex at room temperature.

Molecular docking

The experimental observations were substantiated through molecular docking studies and the preferred binding sites of the ligand and complexes with DNA have been analyzed which plays an important role both in the molecular recognition of the nucleic acid as well as in the rational design of new chemotherapeutic drugs [55]. In our experiment, molecular modelling of ligand (H^2L), copper complexes (**2**, **6** and **8**) and silver complexes (**9** and **10**) with DNA were performed using the AutoDock program, in order to predict the preferred orientation along with suitable binding sites of the molecules within the DNA duplex for interaction. The optimized cluster was ranked by energy levels in the best conformation of the ligand-DNA

modelled structures, and the minimum binding energies of DNA with the H^2L , **2**, **6**, **8**, **9** and **10** showed -7.1, -8.1, -5.9, -6.4, -6.4 and -5.9 kcal mol⁻¹, respectively (Tables S3, S4 of supplementary material). The binding model of ligand (H^2L), copper complexes (**2**, **6**, and **8**) and silver complexes (**9** and **10**) with DNA (PDB: 1BNA) is shown in Figure 9. H^2L , **2**, **6**, and **8** showed H-bonds formed by NH of the ligand and different base pairs of DNA (Table S5 of supplementary material).

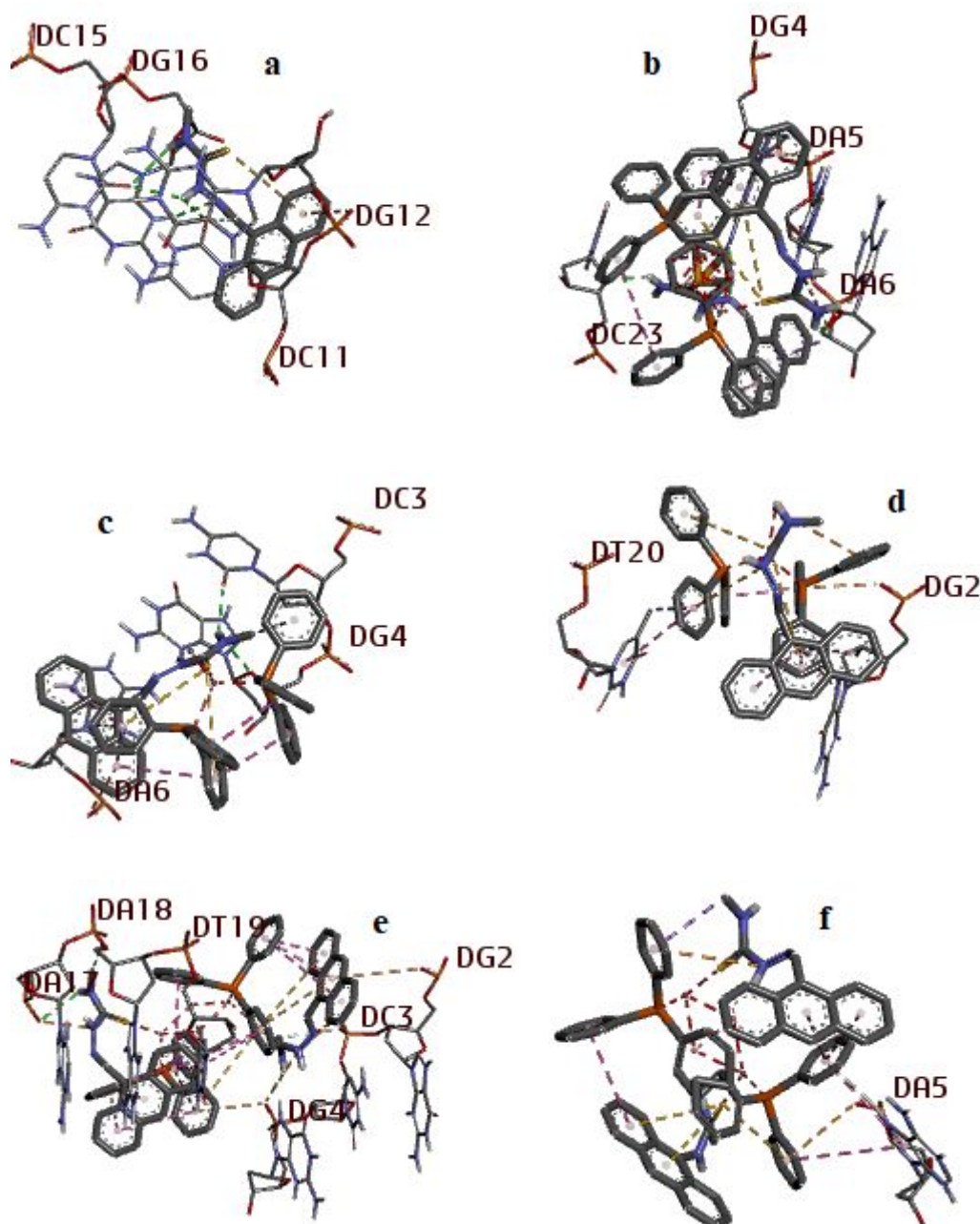


Figure 9. Molecular docking of DNA (1BNA) with compounds H^2L (a), and complexes **2** (b); **6** (c); **8** (d); **9** (e) and **10** (f) obtained using Discovery Studio.

Table 5. Crystallographic data of complexes **2**, **5**, **6** and **9**

	2	5	6	9
Empirical formula	$C_{68}H_{56}Br_2Cu_2N_6P_2S_2$	$C_{68}H_{56}Ag_2Br_2N_6P_2S_2$	$C_{53}H_{45}ClCuN_3P_2S$	$C_{70}H_{60}Ag_2Cl_2N_6P_2S_2$
Formula weight	1370.14	1458.81	916.91	1397.94
Temperature/ K	173(2)	173(2)	173(2)	173(2)
Crystal system	Triclinic	Triclinic	Triclinic	Triclinic
Space group	P-1	P-1	P-1	P-1
a/Å	10.6214(6)	10.7472(4)	9.3618(6)	10.4921(7)
b/Å	11.2972(5)	11.3854(4)	13.0317(6)	12.0020(6)
c/Å	13.7145(7)	13.6865(6)	19.9761(11)	13.8200(10)
α/°	72.608(4)	72.550(4)	87.840(4)	82.287(5)
β/°	70.363(5)	72.019(4)	83.721(5)	79.882(6)
γ/°	75.468(4)	75.693(3)	84.866(5)	75.133(5)
Volume/Å³	1458.20(14)	1497.39(11)	2411.8(2)	1648.60(19)
Z	1	1	2	1
ρ_{calc}/cm^3	1.560	1.618	1.263	1.408
μ/mm^{-1}	2.275	2.160	2.467	6.912
F(000)	696.0	732	952.0	712.0
Crystal size/mm³	0.51 × 0.25 × 0.23	0.55 × 0.31 × 0.18	0.31 × 0.29 × 0.24	0.38 × 0.18 × 0.12
Radiation	MoK α (λ = 0.71073)	MoK α (λ = 0.71073)	CuK α (λ = 1.54184)	CuK α (λ = 1.54184)
2θ range for data collection/°	5.93 to 65.652	3.43- 32.37	6.82 to 142.94	6.526 to 142.5
Index ranges	-15 ≤ h ≤ 15, -16 ≤ k ≤ 17, -20 ≤ l ≤ 20	-16 ≤ h ≤ 15, -17 ≤ k ≤ 17, -20 ≤ l ≤ 20	-11 ≤ h ≤ 11, -16 ≤ k ≤ 15, -21 ≤ l ≤ 24	-12 ≤ h ≤ 12, -14 ≤ k ≤ 10, -16 ≤ l ≤ 16
Reflections collected	17833	19674	17563	11774

Independent reflections	9606 [$R_{\text{int}} = 0.0353$, $R_{\text{sigma}} = 0.0582$]	9887 [$R_{\text{int}} = 0.0375$, $R_{\text{sigma}} = 0.0614$]	9186 [$R_{\text{int}} = 0.0443$, $R_{\text{sigma}} = 0.0543$]	6261 [$R_{\text{int}} = 0.0304$, $R_{\text{sigma}} = 0.0411$]
Data/restraints/parameters	9606/0/370	9887/0/370	9186/0/551	6261/0/380
Goodness-of-fit on 7	1.026	1.025	1.031	1.002
Final R indexes [$I \geq 2\sigma(I)$]	$R_1 = 0.0395$, $wR_2 = 0.0803$	$R_1 = 0.0614$, $wR_2 = 0.0858$	$R_1 = 0.0431$, $wR_2 = 0.1124$	$R_1 = 0.0382$, $wR_2 = 0.0964$
Final R indexes [all data]	$R_1 = 0.0630$, $wR_2 = 0.0913$	$R_1 = 0.0375$, $wR_2 = 0.0749$	$R_1 = 0.0487$, $wR_2 = 0.1177$	$R_1 = 0.0436$, $wR_2 = 0.0997$

Table 6. Important bond lengths (Å) and bond angles (°) of **2**, **5**, **6** and **9**

[Cu ₂ (μ ₂ -Br) ₂ (η ¹ -S-9-Hanttsc) ₂ (Ph ₃ P) ₂] (2)			
Br(1) – Cu(1)	2.4735(4)	Cu(1) – P(1)	2.2469(6)
Br(1) – Cu(1)	2.5909(4)	S(1) – C(1)	1.704(2)
Cu(1) – Br(1)	2.5909(4)	N(1) – N(2)	1.385(2)
Cu(1) – S(1)	2.3360(6)	N(1) – C(1)	1.332(3)
Cu(1) – Br(1) – Cu(1)	76.063(12)	P(1) – Cu(1) – Br(1)	108.23(2)
Br(1) – Cu(1) – Br(1)	103.939(12)	P(1) – Cu(1) – Br(1)	115.876(19)
S(1) – Cu(1) – Br(1)	116.817(19)	P(1) – Cu(1) – S(1)	107.18(2)
S(1) – Cu(1) – Br(1)	103.773(19)	C(1) – S(1) – Cu(1)	113.98(7)
[Ag ₂ (μ ₂ -Br) ₂ (η ¹ -S-9-Hanttsc) ₂ (Ph ₃ P) ₂] (5)			
Ag(1) – Br(1)	2.8086(3)	Br(1) – Ag(1)	2.8086(3)
Ag(1) – Br(1)	2.6534(3)	S(1) – C(1)	1.696(2)
Ag(1) – S(1)	2.5832(6)	N(1) – N(2)	1.385(2)
Ag(1) – P(1)	2.4455(6)	Ag(1) – Ag(1)	3.1774(4)
S(1) – Ag(1) – Br(1)	112.397(15)	P(1) – Ag(1) – S(1)	105.53(2)
S(1) – Ag(1) – Br(1)	100.045(17)	Ag(1) – Br(1) – Ag(1)	71.079(9)
P(1) – Ag(1) – Br(1)	122.854(17)	C(1) – S(1) – Ag(1)	112.78(8)
P(1) – Ag(1) – Br(1)	104.493(15)	C(1) – N(1) – N(2)	121.17(18)
[CuCl(η ¹ -S-9-Hanttsc-N ¹ -Me)(Ph ₃ P) ₂] (6)			

Cu(1) – Cl(1)	2.3703(4)	Cu(1) – P(2)	2.2839(4)
Cu(1) – S(1)	2.3904(4)	S(1) – C(1)	1.6986(15)
Cu(1) – P(1)	2.2732(4)	P(1) – C(8)	1.8201(16)
Cu(1) – P(2)	2.2839(4)	N(1) – N(2)	1.3746(17)
Cl(1) – Cu(1) – S(1)	107.383(15)	P(2) – Cu(1) – Cl(1)	106.870(15)
P(1) – Cu(1) – Cl(1)	104.716(15)	P(2) – Cu(1) – S(1)	109.633(15)
P(1) – Cu(1) – S(1)	102.067(15)	C(1) – S(1) – Cu(1)	108.66(6)
P(1) – Cu(1) – P(2)	125.060(15)		
[Ag ₂ Cl ₂ (μ ₂ -S-9-Hanttsc-N ¹ -Me) ₂ (Ph ₃ P) ₂] (9)			
Ag(1) – Cl(1)	2.5226(7)	S(1) – Ag(1)	2.7762(7)
Ag(1) – S(1)	2.7761(7)	S(1) – C(16)	1.715(3)
Ag(1) – S(1)	2.6007(7)	N(1) – N(2)	1.397(3)
Ag(1) – P(1)	2.4304(7)		
Cl(1) – Ag(1) – S(1)	102.55(2)	P(1) – Ag(1) – S(1)	120.60(2)
Cl(1) – Ag(1) – S(1)	105.60(2)	P(1) – Ag(1) – S(1)	103.73(2)
S(1) – Ag(1) – S(1)	96.631(19)	Ag(1) – S(1) – Ag(1)	83.368(19)
P(1) – Ag(1) – Cl(1)	122.66(2)	C(16) – S(1) – Ag(1)	112.11(9)

Conclusions

9-anthraldehyde thiosemicarbazone (9-Hantsc, H¹L) formed halogen-bridged dinuclear complexes, [M₂(μ₂-X)₂(η¹-S-9-Hanttsc)₂(Ph₃P)₂] (M = Cu, X = Cl, **1**; Br, **2**; I, **3**; M = Ag, X = Cl, **4**; Br, **5**) with copper(I) and silver (I), in contrast to sulfur-bridged dimers, [Ag₂X₂(μ₂-S-9-Hanttsc-N¹-Me)₂(Ph₃P)₂] (X = Cl, **9**; Br, **10**) of Ag(I) and mononuclear complexes, [CuX(η¹-S-9-Hanttsc-N¹-Me)(Ph₃P)₂] (X = Cl, **6**; Br, **7**; I, **8**) of copper(I) with 9-anthraldehyde-N¹-methyl thiosemicarbazone. The substitution of hydrogen by a methyl group at the N¹ atom of thiosemicarbazone has changed the bonding modes in its silver (I) complexes from halogen-bridging to sulphur-bridging and changed the nuclearity of its copper (I) complexes from dimers to monomers. Results of DNA interaction of complexes showed that copper complex **2** showed the strongest interactions with ct-DNA with a binding constant value of 6.66 × 10⁴ M⁻¹, which is 4-5 times higher than that of ligand (**H²L**). Complex **2** also showed strong interactions with HSA with a binding constant value of 3.28 × 10⁴ M⁻¹. The results of DNA and HSA binding for the ligand and complexes showed the binding interactions in the order of **2** > **6** > **8** > **9** > **10** > **H²L**. When tested in various cancer

cell lines, complexes **4** and **9** were found to be most potent in terms of anti-cancer activities since they showed minimum IC₅₀ values in MTT assay in most of the cell lines as tested by us. However, based on this data further in vivo validation of these complexes are needed to appreciate their anti-cancer properties.

Acknowledgements

Crystallographic data for the structural analysis of complexes **2**, **5**, **6** and **9** have been deposited with Cambridge Crystallographic Data Centre, under CCDC No. 2025688, 2025689, 2025690 and 2025691 respectively. Copy of this information may be obtained free of charge from: The Director, CCDC, 12 Union Road, Cambridge CB2 1EZ, UK (fax: 44-1223-336-033; Email: deposit@ccdc.cam.ac.uk; or <http://www.ccdc.cam.ac.uk>). Jerry P. Jasinski expresses thanks to the National Science Foundation Major Research Instrumentation Program 93 (Grant Number CHE-1039027) for funds to purchase an X-ray diffractometer.

References:

1. N.A. Mohamed, R.R. Mohamed, R.S.Seoudi, *Int. J. Biol. Macromol.*, 2014, 63, 163.
2. M.M. Aly, Y.A. Mohamed, K.A.M. El-Bayouki, W.M. Basyouni, S.Y. Abbas, *Eur. J. Med. Chem.*, 2010, 45, 3365.
3. U. Kulandaivelu, V.G. Padmini, K. Suneetha, *Archiv der Pharmazie*, 2011, 344, 84.
4. Y. Yu, D.S. Kalinowski, Z. Kovacevic, *J. Med. Chem.*, 2009, 52, 5271.
5. R.K. Agarwal, L. Singh, D.K. Sharma, *Bioinorg. Chem. Appl.*, 2006, 10.
6. S. Arora, S. Agarwal, S. Singhal, *Int. J. Pharm. Pharmaceut. Sci.*, 2014, 6, 34.
7. N. Parul, N. Subhangkar, M. Arun, *Int. Res. J. Pharm.*, 2012, 3, 351.
8. Z.A. Kaplancikli, M.D. Altintop, B. Sever, Z. Cantürk, A. Özdemir, *J. Chem.* (2016) 7.
9. F.R. Pavan, P.I. da S. Maia, S.R.A. Leite, V.M. Deflon, A.A. Batista, D.N. Sato, S.G.Franzblau,C.Q.F.Leite, *Eur. J. Med. Chem.*, 2010, 45, 1898.
10. T.S.Lobana, R.Sharma, G.Bawa, S.Khanna, *Coord.Chem.Rev.*, 2009, 253, 977.

11. M.A.Ali, S.E.Livingstone, *Coord. Chem. Rev.*, 1974, 13, 115.
12. M.J.M.Campbell, *Coord.Chem.Rev.*, 1975, 15, 279.
13. S.Padhye, G.B.Kauffman, *Coord.Chem.Rev.*, 1985, 63, 127.
14. D.X.West, S.Padhye, P.B.Sonawane, *Struct. Bonding*, 1991, 76, 4.
15. D.X.West, A.E.Liberta, S.Padhye, R.C.Chilkate, P.B.Sonawane, A.S.Kumbhar, R.G.Yerande, *Coord.Chem.Rev.*, 1993, 123, 49.
16. J.S.Casas, M.S.Garcia-Tasende, J.Sordo, *Coord.Chem.Rev.*, 2000, 209, 197.
17. J.S.Casas, M.S.Garcia-Tasende, J.Sordo, *Coord.Chem.Rev.*, 1999, 193, 283.
18. R.K.Mahajan, T.P.S.Walia, T.S.Lobana, Sumanjit, *Anal.Sci.*, 2006, 22, 389.
19. R.K.Mahajan, I.Kaur, T.S.Lobana, *Talanta*, 2003, 59, 101.
20. R.K.Mahajan, T.P.S.Walia, Sumanjit, T.S.Lobana, *Talanta*, 2005, 67, 755.
21. R.K.Mahajan, R.Kaur, T.S.Lobana, *Ind.J.Chem.* 2006, A45, 639.
22. A.Castiñeiras, N.Fernández-Hermida, I.García-Santos, L.Gómez-Rodríguez, *Dalton Trans.* 2012, 41, 13486.
23. M.Hakimi, R.Takjoo, A.Gholami, T.Tabari, *J. Mat. Sci. and Eng.* 2011, B1, 759.
24. Ş.Güveli, S.A.Çınar, Ö.Karahan, V.Aviyente, B.Ülküseven, *Eur. J. Inorg.Chem.* 2016, 4, 538.
25. S.Priyarega, P.Kalaivani, R.Prabhakaran, T.Hashimoto, A. Endo, K.Natarajan, *J. Mol. Strut.*, 2001, 1002, 58.
26. D.Sharma, J.P.Jasinski, V.A.Smolinski, M.Kaur, K.Paul, R.Sharma, *Inorg. Chim. Acta*, 2020, 499, 119187.
27. A.Khan, J.P.Jasinski, V.A.Smolenski, E.P.Hotchkiss, P.T. Kelley, Z.A.Shalit, M.Kaur, K.Paul, R.Sharma, *Bioorg. Chem.*, 2018, 80, 303.
28. R.W.-Y. Sun, D.-L. Ma, E. L.-M. Wong, C.-M. Che, *Dalton Trans.*, 2007, 43, 4884.

29. K. L. Haas, K. J. Franz, *Chem. Rev.*, 2009, 109, 4921.
30. M. S. More, P. G. Joshi, Y. K. Mishra, P. K. Khanna, *Materials Today Chemistry* 2019, 14, 100195.
31. S. P. Fricker, *Dalton Trans.*, 2007, 43, 4903.
32. E. Meggers, *Chem. Comm.*, 2009, 9, 1001.
33. F. A. Beckford, G. Leblanc, J. Thessing, M. Shaloski, Jr. B. J. Frost, L. N. P. Seeram, *Inorg. Chem. Comm.*, 2009, 12, 1094.
34. G. Brauer, *Handbook of Preparative Chemistry*, second ed., Academic Press, New York, 1965.
35. A. Verma, A. K. Varshney, *Int. J. Pharm. Sci. Rev. Res.*, 2015, 30, 18.
36. S. M. Sheldrick, *Crystal structure refinement with SHELXL*, *Acta Cryst.*, 2015, A71, 3.
37. G. M. Sheldrick, *A short history of SHELX*, *Acta Cryst.*, 2008, A64, 112.
38. A. J. C. Wilson, *International Tables for Crystallography*, Kluwer Academic Publishers, Dordrecht, The Netherlands, 1995.
39. M. C. S. Lourenco, M. V. N. de Souza, A. C. Pinheiro, M. de L. Ferreira, R. B. Goncalves, T. Cristina, M. Nogueira, M. A. Peralta, *ARKIVOC*, 2007, 181.
40. H. A. Benesi, J. H. Hildebrand, *J. Am. Chem. Soc.*, 1949, 71, 2703.
41. M. R. Eftink, C. A. Ghiron, *Anal. Biochem.*, 1981, 114, 199.
42. (a) I. Parveen, P. Khan, S. Ali, I. Md. Hassan, N. Ahmed, *Eur. J. Med. Chem.* 2018, 159, 166. (b) P. Bourassa, S. Dubeau, G. M. Maharvi, A. H. Fauq, T. J. Thomas, H. A. Tajmir-Riahi, *Eur. J. Med. Chem.* 2011, 46, 4344.
43. T. Sarwar, M. A. Husain, S. Ur Rehman, H. M. Ishqi, M. Tabish, *Mol. Biosyst.*, 2015, 11, 522.
44. Z. Wu, F. Delaglio, N. Tjandra, V. B. Zhurkin, A. Bax, *J. Biomol. NMR*, 2003, 26, 297.
45. S. Fortli, R. Huey, M. E. Pique, M. Sanner, D. S. Goodsele, A. J. Olson, *Nat. Protoc.*,

- 2016, 11, 905.
46. T.S. Lobana, Rekha, R.J. Butcher, A. Castineiras, E. Bermejo, P.V. Bharatam, *Inorg. Chem.*, 2006, 45, 1535.
 47. R.Sharma, T.S. Lobana, A. Castineiras, R.J. Butcher, T. Akitsu, *Polyhedron*, 2019, 158 449.
 48. T.S. Lobana, S. Khanna, R. Sharma, G. Hundal, R. Sultana, M. Chaudhary, R. J. Butcher, A. Castineiras, *Cryst. Grow. & Des.*, 2008, 8, 1203.
 49. J.E. Huheey, R.L. Keiter, *Inorganic Chemistry; Principal of Structure and Reactivity*, 4th ed., Harper Collins College Publishers, New York, 1993.
 50. L. Pauling, *The Nature of the Chemical Bond*, 3rd ed., Cornell University Press, New York, 1960.
 51. F.R. Pavan, P.I. da S. Maia, S.R.A. Leite, V.M. Deflon, A.A. Batista, D.N. Sato, S.G.Franzblau,C.Q.F.Leite, *Eur. J. Med. Chem.*, 2010, 45, 1898.
 52. R. Hajian, P. Hossaini, Z. Mehrayin, P. M. Woi, N. Shams, *J. Pharm. Anal.*, 2017, 7, 176.
 53. J. B. Lepecq, C. A. Paoletti, *J. Mol. Biol.* 1967, 27, 87.
 54. F.A. Beckforda, A. Brock, A. Gonzalez-Sarrías, N.P. Seeram, *J Mol Struct.* 2016, 1121, 156.
 55. J. R. Lakowicz, G. Webber, *Biochem.*, 1973, 12, 4161.